SANDIA REPORT

SAND 2006-6203
Unlimited Release
Printed May 2007

Contamination and Solid State Welds

Bernice E. Mills

Prepared by
Sandia National Laboratories
Albuquerque, New Mexico 87185 and Livermore, California 94550

Sandia is a multiprogram laboratory operated by Sandia Corporation,
a Lockheed Martin Company, for the United States Department of Energy's
National Nuclear Security Administration under Contract DE-AC04-94-AL85000.

Issued by Sandia National Laboratories, operated for the United States Department of Energy by Sandia Corporation.

Available to DOE and DOE contractors from
U.S. Department of Energy
Office of Scientific and Technical Information
P.O. Box 62
Oak Ridge, TN 37831

Telephone: (865) 576-8401
Facsimile: (865) 576-5728
E-Mail: reports@adonis.osti.gov
Online ordering: http://www.doe.gov/bridge

Available to the public from
U.S. Department of Commerce
National Technical Information Service
5285 Port Royal Rd
Springfield, VA 22161

Telephone: (800) 553-6847
Facsimile: (703) 605-6900
E-Mail: orders@ntis.fedworld.gov
Online order: http://www.ntis.gov/help/ordermethods.asp?loc=7-4-0#online

SAND 2006-6203
Unlimited Release
Printed May 2007

Contamination and Solid State Welds

Bernice E. Mills
Materials Chemistry Department
Sandia National Laboratories
P.O. Box 969
Livermore, California-9403

Abstract

Since sensitivity to contamination is one of the verities of solid state joining, there is a need for assessing contamination of the part(s) to be joined, preferably nondestructively while it can be remedied. As the surfaces that are joined in pinch welds are inaccessible and thus provide a greater challenge, most of the discussion is of the search for the origin and effect of contamination on pinch welding and ways to detect and mitigate it. An example of contamination and the investigation and remediation of such a system is presented. Suggestions are made for techniques for nondestructive evaluation of contamination of surfaces for other solid state welds as well as for pinch welds. Surfaces that have good visual access are amenable to inspection by diffuse reflection infrared Fourier transform (DRIFT) spectroscopy. Although other techniques are useful for specific classes of contaminants (such as hydrocarbons), DRIFT can be used most classes of contaminants. Surfaces such as the interior of open tubes or stems that are to be pinch welded can be inspected using infrared reflection spectroscopy. It must be demonstrated whether or not this tool can detect graphite-based contamination, which has been seen in stems. For tubes with one closed end, the technique that should be investigated is emission infrared spectroscopy.

This page intentionally left blank.

Contents

This page intentionally left blank.

List of Figures

This page intentionally left blank.

Contamination and Solid State Welds

Solid State Welds

Solid state joints include resistance, friction, and diffusion welds and electroplated joints. Both pinch welds and forge welds are resistance heated. There are advantages and disadvantages to resistance solid-state welds.

Because solid state welding does not change the material composition, there is no strength loss and compatibility is generally not compromised. Further, it is easier to control the dimensions and residual stresses of the component. Generally, solid state welds are quicker and easier to develop than fusion welds—and weld development time can be a schedule driver. Finally, solid state joining can be less costly and less operator dependent than other joining techniques. Unfortunately, solid-state welds are not repairable and are sensitive to contamination. It is this latter property that will be addressed with respect to pinch welds.

Pinch Welds

Pinch welds are performed on gas bottles used for tritium, deuterium, and working fluids. They are also used to seal off pits and secondaries. The latter systems use tubing, which is very well characterized and controlled. Because of this they have little concern with contamination and do not need to inspect each part. On the other hand, gas bottles for tritium are often made from forgings, which are gun or peck drilled to produce an integral stem. This produces a very robust system for high pressure hydrogen isotope applications, but also introduces the possibility of contamination introduced during the drilling process.

Contamination Observations

Historically there have been observations of contamination likely introduced during stem drilling at Rocky Flats. After close examination of gun drilled stems and pinch welds produced during qualification of new pinch welding stations in the 1990s, it was observed that some of the stems had significant amounts of contamination that was incorporated into the weld, Figure 1.

Figure 1. **Examples of pinch welds made using contaminated stems.**

Note that although there are extensive indications of contamination included at the bond line, there is also grain growth at the bond line where there is no contamination, indicating good solid state bonding at those areas.

For examples of classification of quality of pinch welds see Appendix A [1]. Some stems were cut open for identification of the contaminants by optical and secondary electron (SEM) imaging and by Auger electron spectroscopy, including mapping and depth profiling.

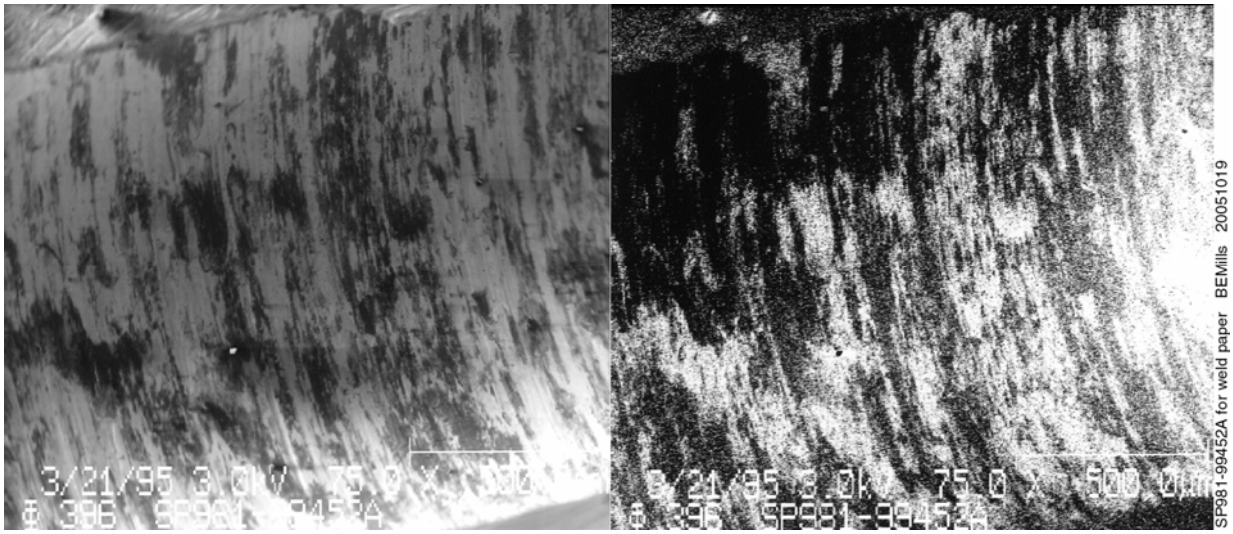

Figure 2. **Images of interior of sectioned SP981 stem 99452A. The dark patches in the secondary image at left and the light patches in the corresponding carbon Auger image at right are thick, adherent contamination that is resistant to hot nitric acid/Nitradd cleaning.**

An example (Figure 2) [2] shows that the darker areas in the SEM image are heavy in carbon in the Auger image.

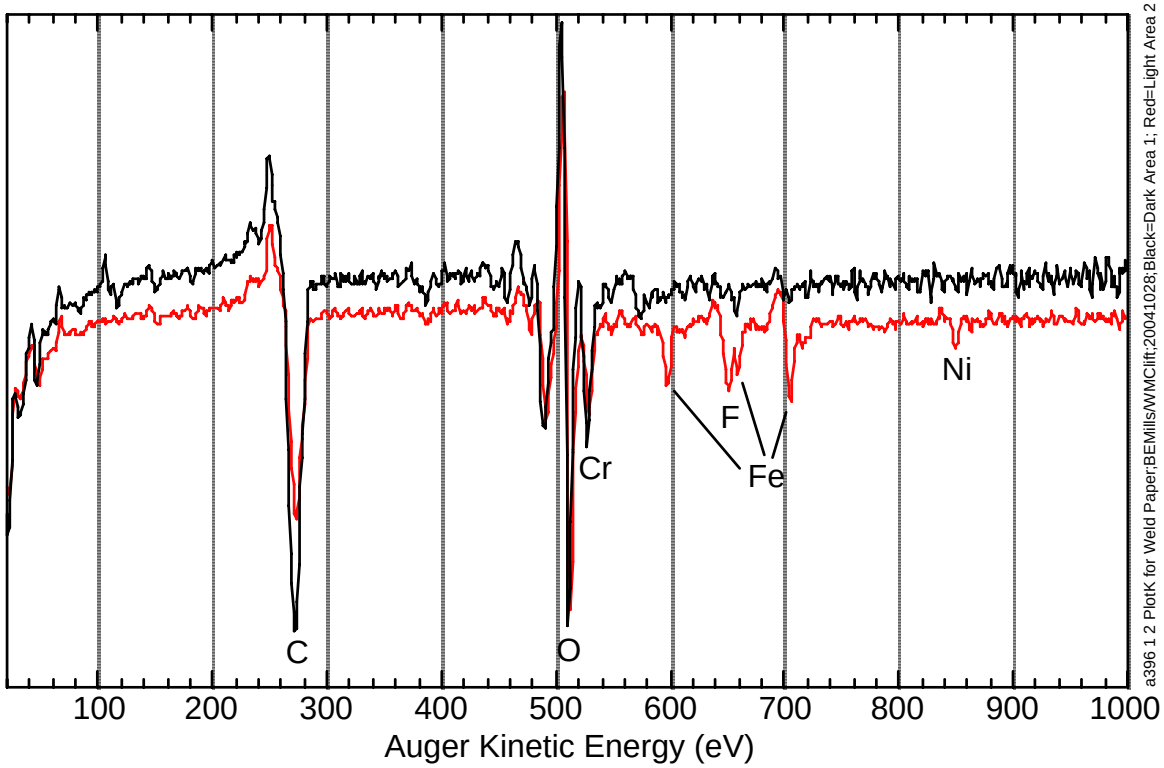

Figure 3. **Auger spectra of section of stem shown in Figure 1 red line (bottom) represents an area that is light in the secondary image and, in addition to the metal components Fe, Ni, and Cr, the typical surface oxide, and the adventitious carbon, shows the tell-tale fluoride peak left by the nitric/Nitradd cleaning and passivation process. The black line (top) represents an area that is black in the secondary electron image where the Fe is barely visible, but the Cr and C is enriched.**

An examination of the areas that appear light and dark by Auger spectroscopy (Figure 3) indicates that the stem has been nitric/Nitradd cleaned, as required, because that process leaves behind the tell-tale fluoride signature that indicates that the surface has been cleaned and passivated but the dark areas survived the nitric/Nitradd process. Several areas on this surface were depth profiled in the Auger. Figure 4 shows a typical light or "clean" area and a typical dark or contaminated area. Although the "clean" area might have a superficial oxide and surface coat of adventitious carbon, the dark areas have a much thicker (on the order of one micron or more) uniform deposit of carbon and oxide. This carbon is graphitic rather than a hydrocarbon or carbide. The oxide is enriched in chromium (implying a near-surface region depleted of chromium). It was concluded that a sufficient amount of this contaminant would compromise the quality of the pinch welds in these stems.

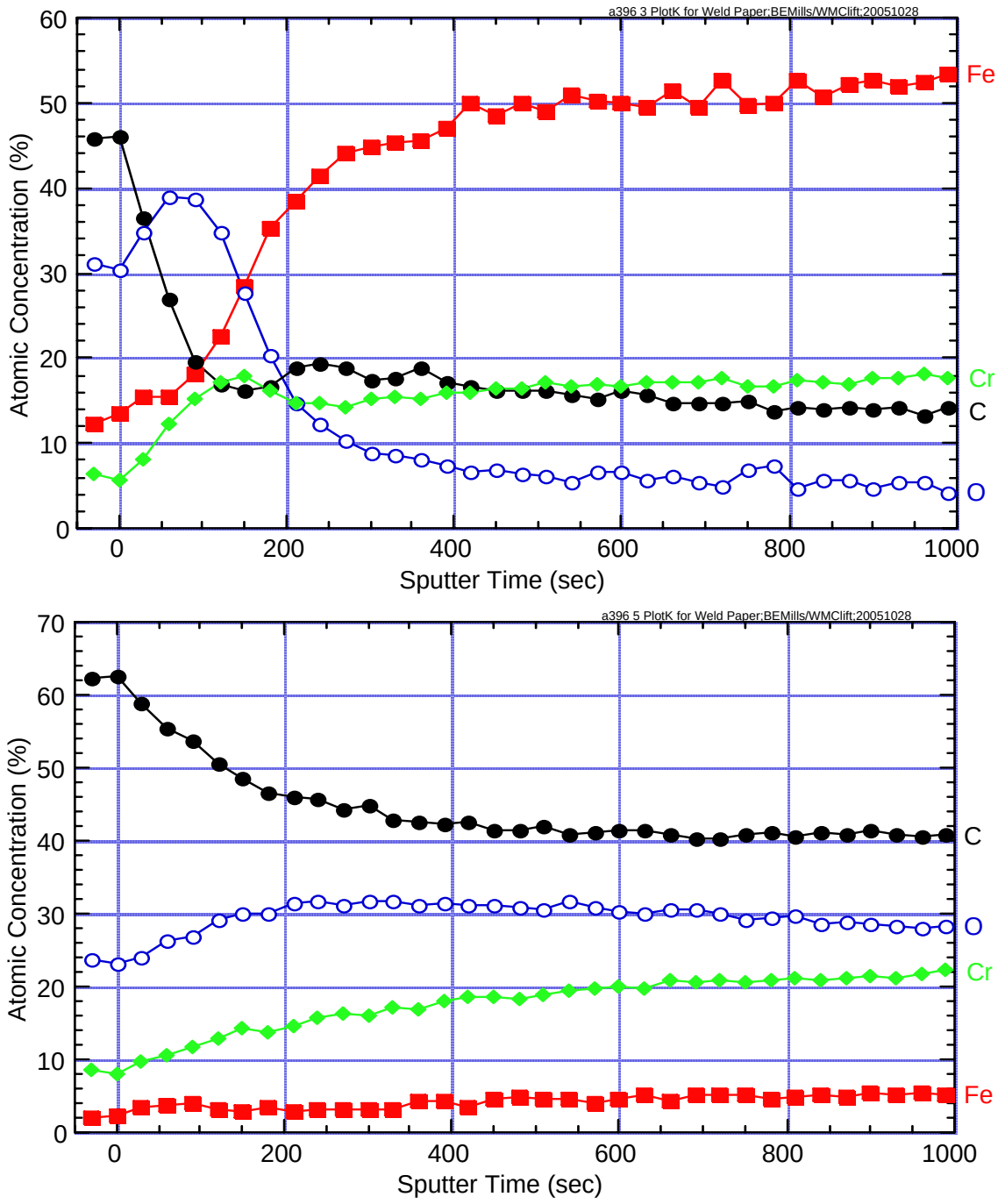

Figure 4. **Auger depth profile of two areas of contaminated stem shown in Figure 1 and 2. Top is typical of the "clean" light areas with a thin adventitious C layer over a thin oxide that is slightly depleted in Fe (the nitric/Nitradd process strips the Fe selectively) and slightly enriched in Cr. The C and O signals persist because the rough surface is not all exposed to the ion beam, which is used to sputter away material. Bottom is typical of the dark areas where, beneath the adventitious C layer, is a layer of carbon mixed with chromium oxide.**

Identify Cause of Contamination

A program to identify the root cause of this contamination was instituted. A program was also started to develop a technique to detect this contamination nondestructively (non-destructive evaluation, or NDE). And a program was initiated to develop a process for removing the contamination from already contaminated stems. Each of these goals (root cause, NDE, and removal) would benefit from reproducing the contamination during gun drilling. So a series of experiments was performed after interviewing the people most familiar with the drilling process at Rocky Flats.

Information from Rocky Flats

The Rocky Flats staff explained that the cutting fluid used was chosen so that they could use the same equipment to drill not only our steel stems, but also copper. As such it was not the optimum that would have been chosen to gun drill only steel. They also stated that they had observed occasional intermittent loss of coolant flow through the drill bit, which is actively cooled through the use of a hole down the center of the drill (Figure 5) and that the cutting fluid had not been changed for several years during the time that the contaminated stems were fabricated. They also reported that drilling longer stems was more problematic than drilling shorter ones—there was more likelihood of drill breakage, for example. This information confirmed the suspicion that the root cause of the contamination was related to the drilling procedure. They also suggested that a different drill bit tip geometry (duboff angle or primary cut angle) might be related to coolant flow blockage, and thus heating of the metal in contact with the drill bit.

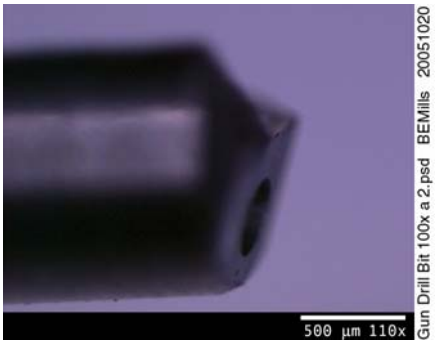

Figure 5. **Image of the tip of a gun drill bit showing the hole through the center of the bit through which high pressure oil is pumped to cool the bit and work piece and to flush out cutting chips. Gun drill bits are solid carbide, which is stiffer. Peck drill bits are made from carbide tips brazed to steel, which makes them tougher but more subject to breakage.**

Oil Degradation

Although it was not possible to obtain the original cutting fluid that had been used during manufacture of the contaminated stems and was not changed for several years at a time, one year old oil was available for comparison with new oil. A comparison of the Fourier transform infrared (FTIR) spectra of old and new samples of oil indicates significant changes, including some oxidation, shown in Figure 6, top, along with a spectrum from the test stems described below). The peak at 1725 cm-1 is characteristic of the C=O stretch of an aldehyde (RCHO) or a carboxylic acid (RCOOH).

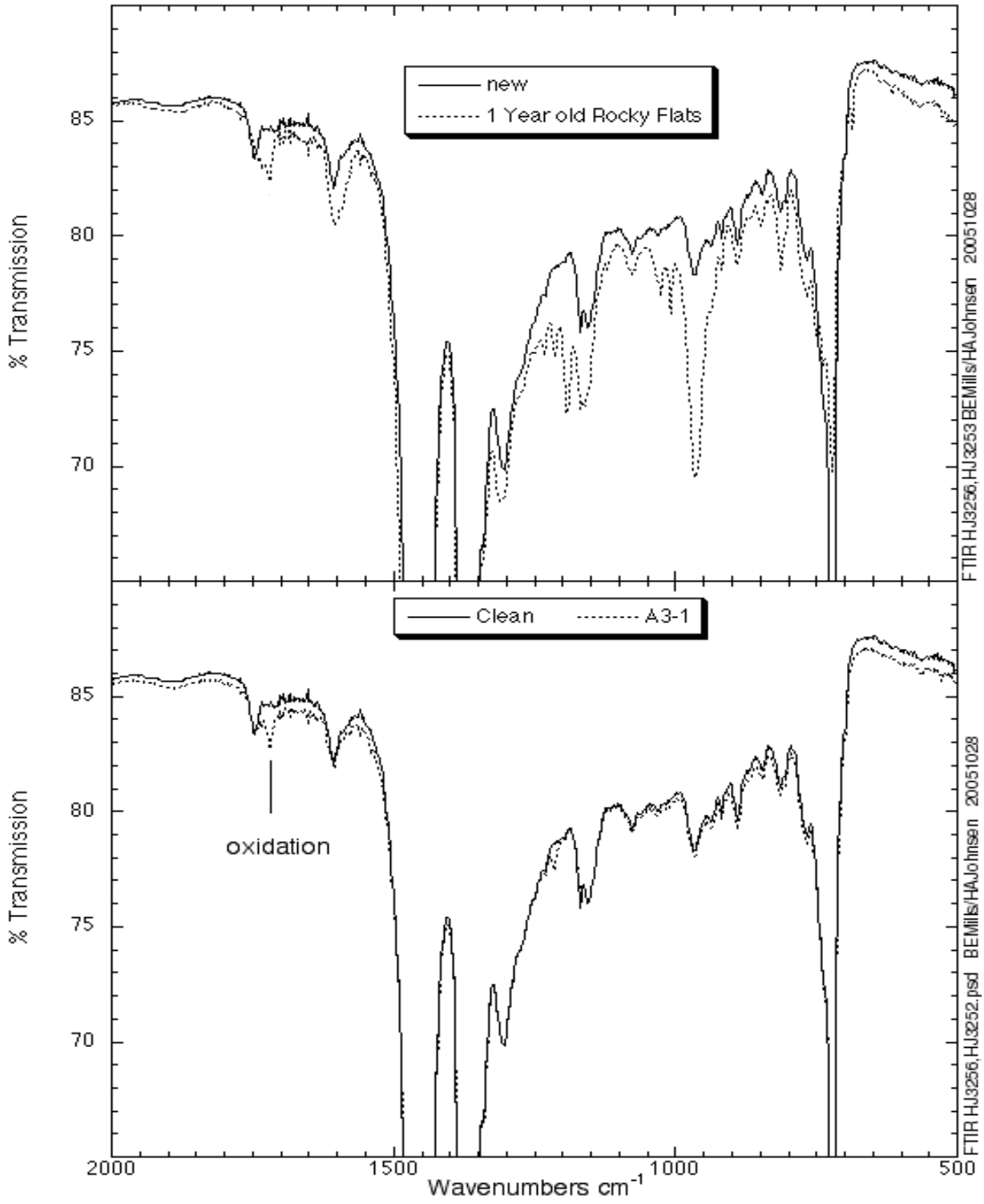

Figure 6. **FTIR spectra of new (clean) oil compared with one year old Rocky Flats oil and with oil captured from the exit from the part during the parametric gun drilling study summarized in Figure 8.**

Note that oxidation is seen after only short time of use, but the changes are much more extensive after one year of use.

New and aged cutting oil was also compared using thermogravimetric analysis (TGA) (Figure 7). The old oil begins to volatilize well below 100°C and well below that of the new oil. As the oil vaporizes, its heat capacity decreases by up to two orders of magnitude, decreasing the effectiveness of the cooling.

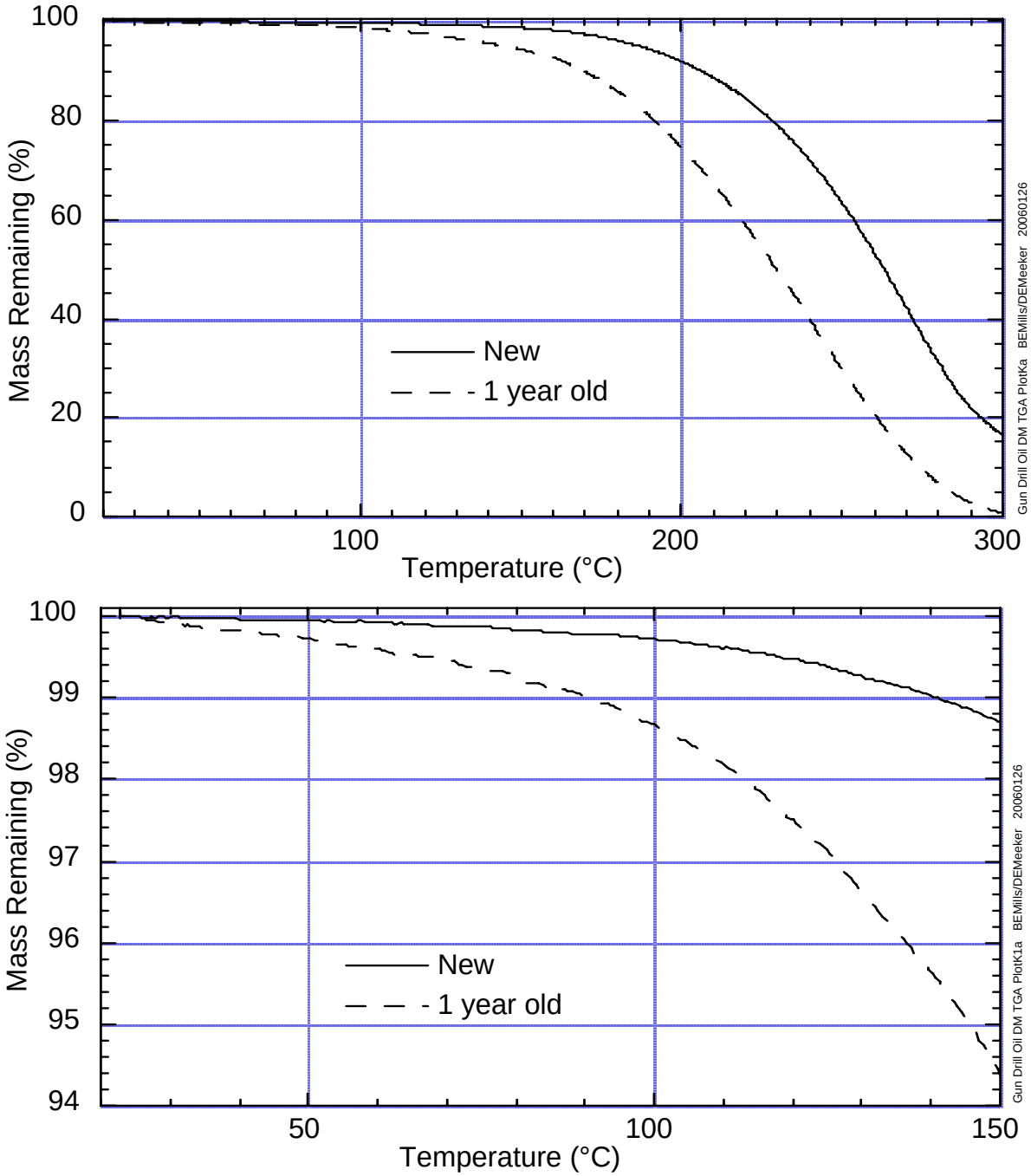

Figure 7. **Thermogravimetric analysis (TGA) of new gun drill oil compared to one year old oil. The bottom shows a blow-up of the first few percent of vaporization. Note that the onset of vaporization begins at very low temperature and continues at up to 50 K lower temperature for the old oil compared to the new oil.**

New and old cutting oil was also compared using size exclusion chromatography (SEC) (Figure 8) [3]. As the average molecular weight of a sample decreases, the retention time in SEC increases. The average retention time for new oil increased from 8.48 to 8.81 for the sample of old oil, indicating a decrease in average molecular weight. The shoulder on the right side of the old oil peak suggests chain breakage.

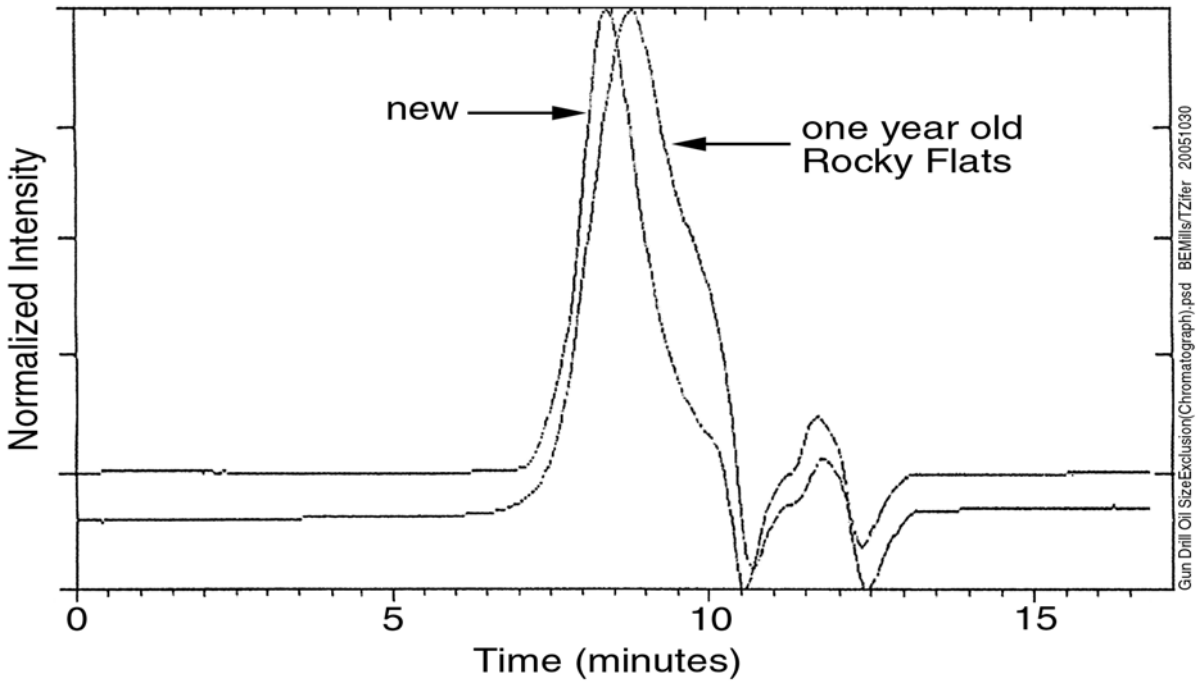

Sample	ID#	Inj#	Retention Time/min
New Oil	5x25xA	1	8.52
		2	8.50
	5x25xE	1	8.46
		2	8.47
	5x25xG	1	8.46
		2	8.46
One Year Old Oil	5x25xB	1	8.82
		2	8.82
	5x25xD	1	8.80
		2	8.81
	5x25xF	1	8.78
		2	8.84
THF Blank (solvent)	5x25xC	1	N/A

Gun Drill Oil SEC tableA.psd BEMills/TZifer 20051030
Gun Drill Oil SEC WeldPaper.psd

Figure 8. **Size Exclusion Chromatography on new and one year old Rocky Flats gun drill oil shows that the average retention time shifts 0.3 minutes longer for the older oil and that there is a pronounced shoulder on the trailing edge of the aged oil peak. Both of these indicate a shift towards lower average molecular weight and chain breakage. Above are typical chromatograms and below is a table of retention times for two injections each for three different samples of each oil, showing excellent reproducibility.**

These techniques for evaluating the oil suggest a mechanism for the oil to fail to perform and several techniques that could be used to quantify the breakdown of the oil and, ultimately, to predict its remaining useful life.

Attempt to Reproduce

In an effort to determine if any gun drill or drilling equipment parameters effect the deposition of contamination and to produce some contaminated stems for subsequent experiments, several series of test drills was performed varying such parameters as the feed rate, spindle speed, oil pressure, duboff angle, and primary cutting angle. Tests were done using gun drilling and peck drilling, with the latter varying the peck drill depth. Also reported was the drilling depth and the number of drills used. For one series, these tests forgings were also instrumented to measure, in addition to the ambient and oil reservoir temperature, the temperature of the oil as it exited the part and the temperature of the part at the center and end (shown on the small schematics on the data plots of Figure 9). Three sample records of the temperature variation throughout the experiment are shown (Figure 9 A4-19, A3-1, A3-8). All temperatures are shown in °F. A3-8 shows a typical record, where the oil that exits from the part warms slowly to reach a steady state value. The metal temperature rises as the drill bit tip heats the nearby steel. It peaks and then falls only after the tip has passed. As the drill bit tip moves on, the heated oil keeps the zone that has already been drilled warm as it picks up more heat and exits through the entire bored out length.

Gun Drill Data Sheet Date 03/15/95

Duplicate Run No. 1		Equipment Parameters				Gun Drill Data		In - Process Machining Data				
Run Order Number	Sample Number	Feed Rate (IPM)	Spindle Speed (RPM)	Oil Press. (PSI)	G.D. Oil Temp. (deg. F	Duboff Angle (deg.)	PRI Cut Angle (deg.)	Ambient Temp. (deg. F)	Drill Start Time	Drill Thru Time	Drilling Depth & No.of drills used: Depth	1
1	A3-5	0.3C	164C	150C	104	15	25	72	2:4C		.03C	3
2	A4-17	0.3C	455C	150C	108	15	35	71	11:4C		THRU	2
3	A4-7	0.3C	164C	180C	108	15	35	73	12:5C		.525	3
4	A3-12	0.3C	455C	150C	108	30	25	75	3:25		THRU	1
5	A3-4	0.2C	455C	180C	104	15	35	71	8:31		1.60C	2
6	A4-19	0.2C	455C	150C	108	15	25	74	9:57		THRU	1
7	A3-6	0.3C	455C	180C	108	3C	35	74	11:28		THRU	1
8	A3-3	0.2C	455C	180C	11C	30	25	74			THRU	1
9	A4-5	0.3C	164C	150C	11C	30	35	76	2:15		1.60C	1
10	A4-2	0.3C	164C	180C	109	30	25	72	4:0C		0.60C	1
11	A4-10	0.2C	164C	180C	109	15	25	71	11:3C		3.30C	4
12	A3-13	0.2C	164C	150C	108	3C	25	74	2:47		THRU	1
13	A3-9	0.2C	455C	150C	108	3C	35	74	3:5C		THRU	1
14	A3-11	0.2C	164C	180C	108	3C	35	74	4:29		THRU	1
15	A4-3	0.2C	164C	150C	108	15	35	73	5:27		.125	1
16	A3-8	0.3C	455C	180C	104	15	25	74	4:0C		THRU	1
17A	A4-1	0.4C	455C	165C	102	3C	25	71	9:0C		THRU	1
18A	A4-4	0.4C	455C	165C	104	3C	35	72	9:3C		THRU	1
19A	A3-1	0.4C	455C	165C	105	15	25	71	10:05		3.59C	1
20A	A4-12	0.4C	164C	165C	106	3C	25	73	10:5C		0.17E	2

A3 & A4 samples are machined from Acorn forging THRU = 3.60" Sheet 1 of 2 PJR/8414

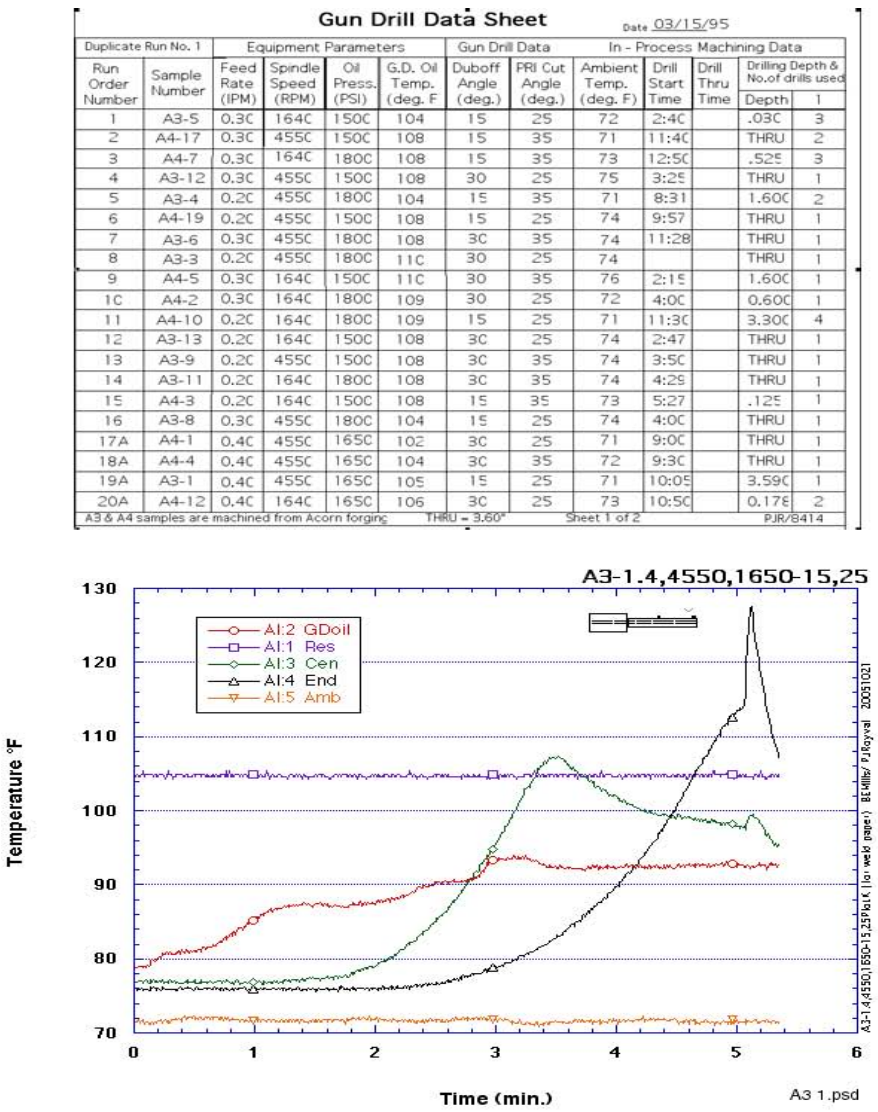

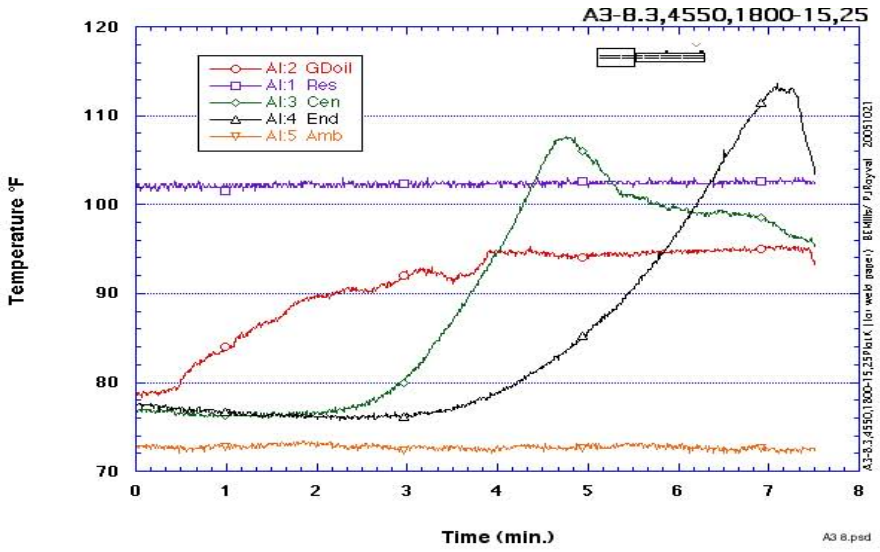

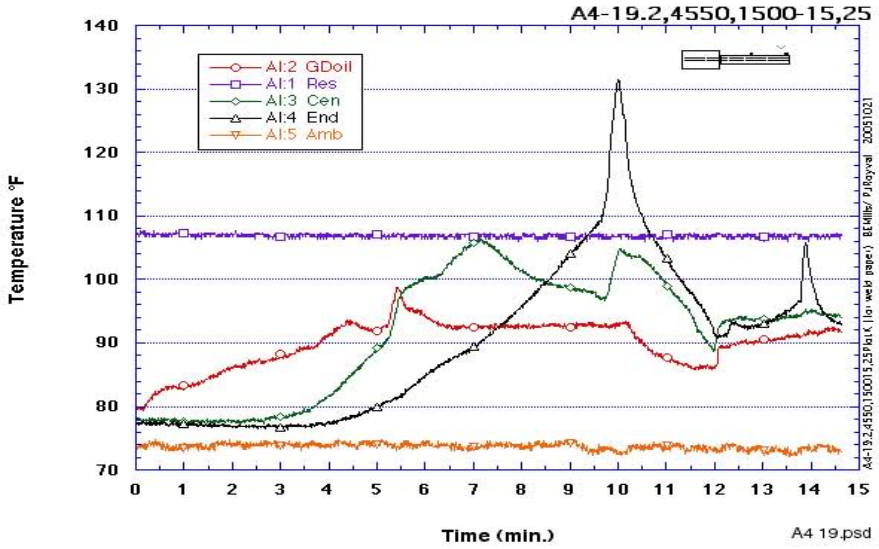

Figure 9. An example of one of the attempts to determine the cause of contaminated stems with some examples of temperatures of the outside of the stem and of the oil. See text for detailed discussion.

A3-1 shows a very similar record until shortly before the drill is about to go through. At that point the temperature of the end shows a pronounced spike. The same temperature spike is recorded by the central thermocouple slightly later and with much less intensity. About a third of the way into the experiment, A4-19 shows a temporary decrease in temperature of the oil exiting the part, followed by a small but sharp increase in the central temperature (recall that the bit has presumably not reached the center thermocouple yet). At about the 2/3 point in the experiment both the central and end temperature measurements spike associated with a decrease in oil temperature. Finally there are small temperature excursions near the end of the drilling that are not reflected in a significant change in oil temperature.

It is clear that it is possible to have a large effect on the material temperature and that this is associated with coolant temperature changes. This is consistent with a scenario where the change in molecular weight of the oil is decreased by thermal excursions and oxidation so that it becomes easier to vaporize. When the oil is vaporized by heat generated when the bit hits a hard spot in the drilling or the coolant flow is temporarily blocked, the localized cooling is completely disrupted as the vapor has very poor thermal capacity compared to the liquid. This allows the local surface temperature to run away and cause:

1) cracking of the remaining liquid oil to deposit graphitic carbon on the surface, and
2) heating the substrate metal to the point where chromium can diffuse to the surface and oxidize to form chromium oxide.

The Fourier transform infrared experiments discussed below indicate the kinds of temperatures that must have been reached, albeit for a much shorter time. N.B., at this temperature carbon can also diffuse out of the bulk to the surface.

Even though the probable cause of the contamination had been identified, these experiments had failed reproduce the contamination observed in actual stems. In order to test any cleaning technique that was to be developed to salvage the contaminated bottles, contaminated stems were needed that did not require sacrifice of valuable components. The final tests would, of course, be made with real parts. At that time we had a program to develop substrate materials in support of a "pre-competitive" multi-company CRADA. The Materials Chemistry group was producing advanced lithium-ion battery turbo-stratic carbons via the thermal decomposition of polymeric starting materials During this process, carbonaceous species were produced which condensed on surfaces within the furnace to produce compact continuous coatings or films. These coatings represented condensed phase equilibrium structure representative of a 1100°C deposition process. [4]. Small quartz tubes of about the dimension of a fill stem were included in experimental runs for this program (Figure 10) [5]. The tubes collected graphite on their interior surface that could then be cleaned off by subsequent treatment (Figure 11). Since they are clear, it is easy to determine the extent of cleaning.

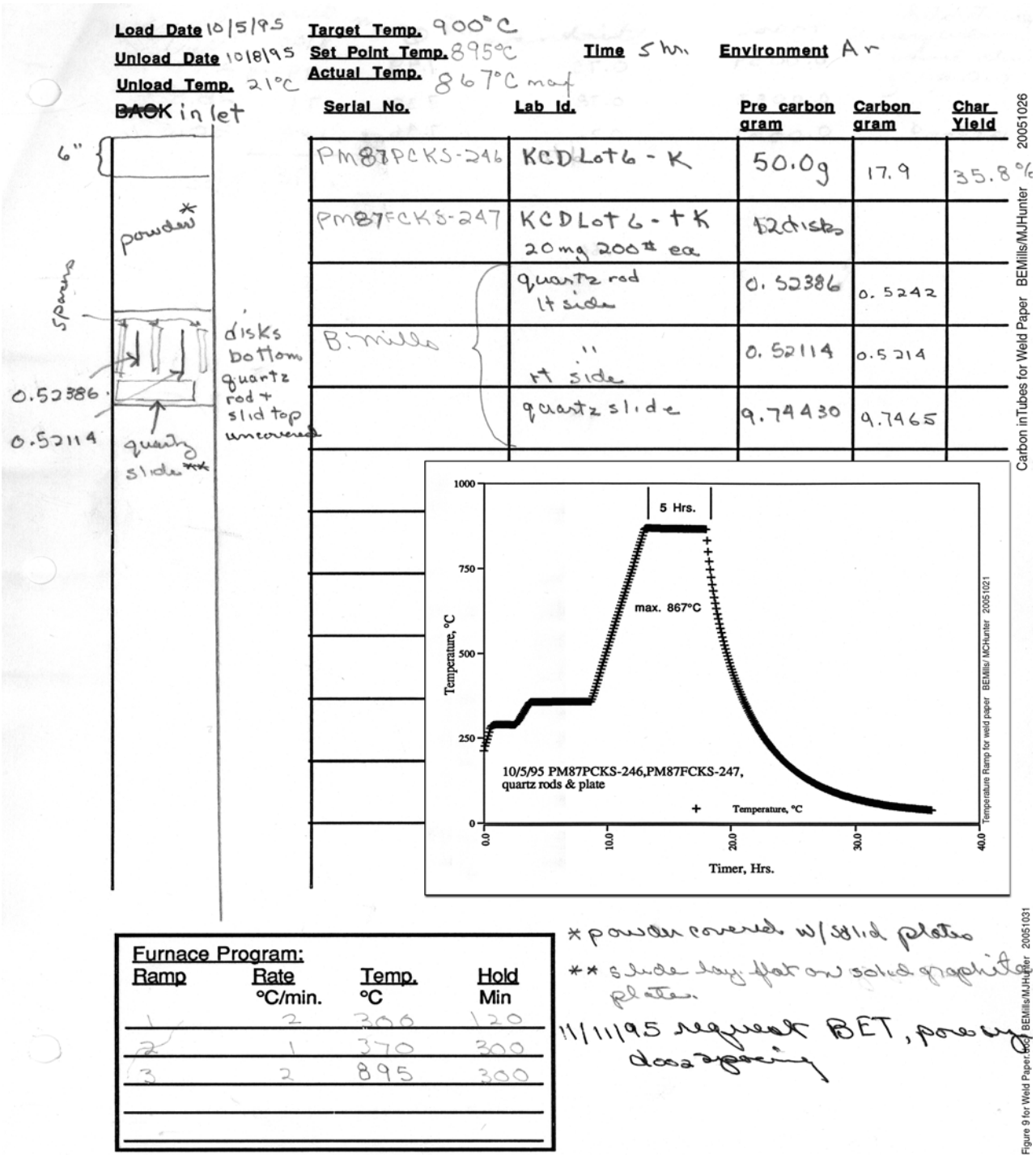

Figure 10. **Example of record of deposition of graphite carbon inside quartz tubes and onto a quartz witness. Diagram of setup of samples and source material in furnace is at left. Temperature record of furnace is shown in inset graph. These experiments allowed us to obtain uniform, known graphite deposits inside tubes for subsequent cleaning experiments.**

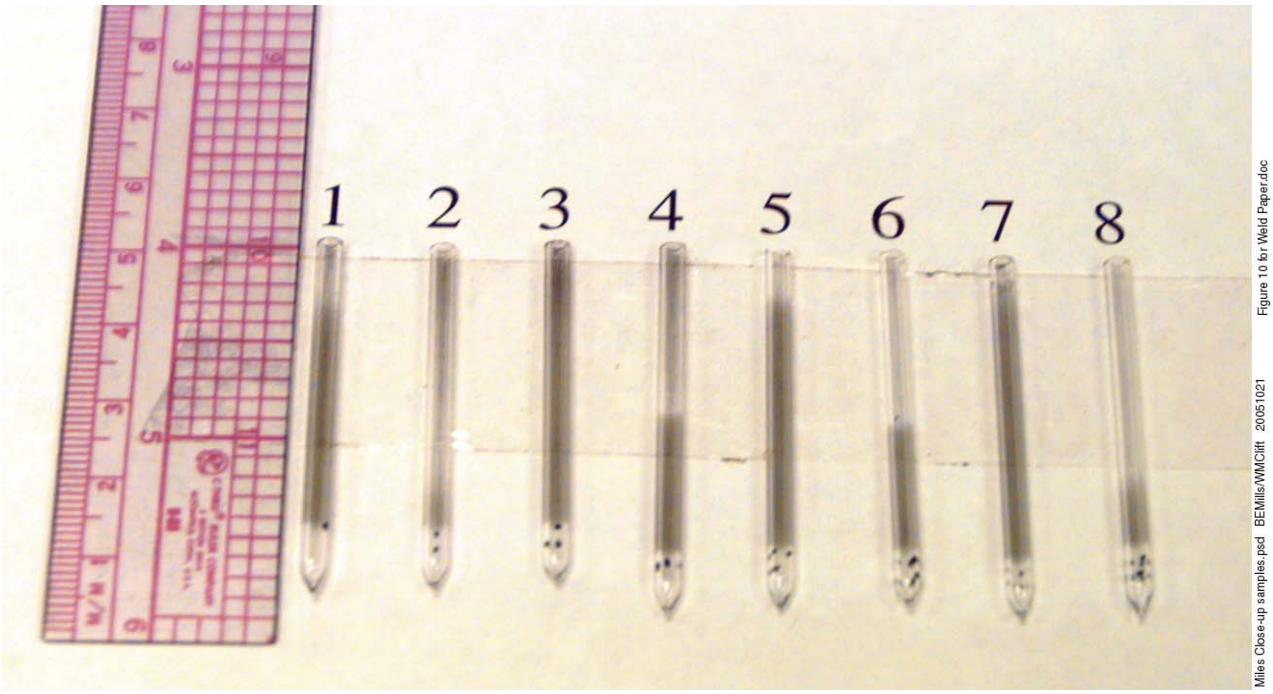

Figure 11. Quartz tubes with graphite deposited in them during the experiments shown in the previous figure were then used for tests of cleaning efficiency for various chemical downstream etching parameters.

Experiments

Appendix B contains excerpts from a report on the effects of various contaminants on pinch welds [6].

Jellison reviewed the role of surface contamination in solid state welding [7]. He discusses inorganic, organic, and particulate contaminants. He includes the effect of welding parameters, atmosphere, and surface condition as well and contaminants.

Recent work [8] compares clean and particulate contaminated pinch welds performed in identical fashion. The contamination (known as tritium facility dust or TFD) was chosen to simulate material that was found on the internal surfaces of several loading lines. It was a mixture of ammonium hexaflurosilicate, calcium silicate powder (-200 mesh), and Teflon® Zonyl® Micronized Powder (4-12μ) that was artificially introduced into the area to be welded at levels far in excess of expected contamination. The material welded was Type 316 and Type 304L stainless steel and 21-6-9 (Nitronic 40) alloy fill stems. All welds were acceptable (Class 1 or 2) and the authors found no evidence that the contamination interfered with the weld quality.

Unfortunately none of these experiments directly addresses the residue of gun drilling.

Experiments to assess cleanliness of surface

In order to examine the interior of pinch weld tubes nondestructively, reflection Fourier transform infrared (FTIR) spectroscopy was used to evaluate nitric/Nitradd cleaned 304L and 316 stainless steel tubes that had been oxidized in air at 500°C, 600°C, or 700°C for one hour. The tubes were either 0.7 mm ID and 25 mm long or 1.0 mm ID and up to 10 cm long. This technique can detect oxides [9] organics and ionic metal salts. It was thought that the only

contaminant of interest that could not be detected was metallic particles. Graphite contamination was not considered. The passivation layer left by the nitric Nitradd cleaning process is too thin to be detected. The oxide layers left by the thermal treatments were all easily detected even though they produced Class 1 or Class 2 welds or welds with expulsion.

Another report [10] also included reflection FTIR studies of organics in stems. It was demonstrated that, for a four minute collection time, the detection limit for aliphatic (i.e. straight chains with no multiple bonds) hydrocarbon oils is on the order of 5 nm thickness in a 0.7 mm diameter, 25 mm long steel tube. Longer collection times would presumably lower the detection limit.

For surfaces destined to be inertial welded, it is possible to map the surface for a contaminant or class of contaminants using tunable infrared laser imaging [11]. The authors studied drawing agent, lubricant, silicone, a couple of mold releases, solder flux and hydraulic oil on surfaces such as aluminum-7075-T6 of different surface finishes, titanium 6Al-4V, Steel Alloy 4340, Stainless Steel 304, and Magnesium AZ31B. They used the spectral signal at 2915 and 3000 wavenumbers (cm^{-1}) to obtain a 256 x 256 pixel image of hydrocarbon contaminants on the surface. They employ continuous wave-optical parametric oscillators (cw OPO) using the quasi-phase matching (QPM) material periodically-poled lithium niobate (PPLN) and an indium antimonide (InSb) focal-plane array (FPA) camera. For typical hydrocarbon species, their detection limit appears to be on the order of 10 to 20 nm film thickness. Unfortunately, for each class of contaminant, it is necessary to develop a new procedure, including determining the appropriate lines to study, obtaining the proper laser source, and calibrating the spectra. Since contamination is never expected, the type of contamination cannot be anticipated, and each type of contaminant could basically require a new instrument to be developed, built, and utilized.

A related technique for detecting a wider variety of contaminants is diffuse reflection infrared (DRIFT) spectroscopy. It can be used to detect organics, oxides, and salts without first knowing what to expect. [12] As such DRIFT is a promising candidate for detecting contamination of accessible surfaces before solid state welding. Metallic contamination cannot be detected by its absorption, but if a characteristic particle size is anticipated, it may be detected by its scattering characteristics. If imaging is used with DRIFT spectra, newer techniques for data analysis such as AXSIA (for Automated eXpert Spectral Image Analysis) should be useful. This tool makes use of multivariate statistical analysis. [13]

Other traditional techniques to measure cleanliness of a surface include contact angle and wetability measurements. These generally are applied to organic contaminants, but would not necessarily be limited to them. Choice of solvent would be directed by what is expected on the surface and the solubility parameter should be considered when picking a solvent. Of course, this is not a non-contact method.

Another alternative is MESERAN measurement (an acronym for Measurement and Evaluation of Surfaces by Evaporative Rate ANalysis), but this is also not a non-contact technique as it requires the use of a solvent and a radioactive tracer deposited on the surface of interest. [14] Again, it is helpful to know the nature of the contaminant in order to choose the proper solvent for the measurement.

For fluorescent species luminescence using ultraviolet excitation can be used, but this is a minor subclass of organic contaminants. If the contaminant species is not fluorescent, it can be made so by derivativization, but this further contaminates the surface. [15]

Electron emission stimulated by UV light is another technique, but it has proven very susceptible to such things as aging and texture of surface in addition to contamination.

Remediation of contamination in stems

Several techniques were considered for removing the graphite-based contamination found in stems parts that were already fabricated. Mechanical reaming was developed but not implemented. In this process the interior of the bottle is protected by a removable polymer plug while the interior diameter of the stem is made slightly larger and then flushed with cleaning solution and rinsed. Although this process worked and it was felt that the larger ID stems could be successfully welded, it was not, in the end, implemented due to the relative complexity of the process. Plasma cleaning was also tried but resulted in heating the part because the ions in the plasma are attracted outer surfaces, particularly edges, by the field lines. These lines do not penetrate into the stem, and so the ions are not effective in cleaning the interior surfaces and, because the part gets hot, oxidation of the base metal is always a concern.

Chemical downstream etching, (CDE, also called for our application downsteam plasma cleaning) is a cleaning technique that can be used to remove carbon without damaging the underlying material. The process starts with a plasma generated in a quartz tube as it would be for plasma cleaning. The ions are then allowed to interact with the walls of the quartz until they are neutralized to reactive atomic and molecular species, to which the surfaces to be cleaned are exposed. Tools that use this technique are usually built to process components built on silicon wafers and have suitable geometries for wafers. Because we had collaborated with a bay area firm to address a materials problem that they had, they kindly let us use their $1,000,000+ tool for some scoping and development tests.

First tested were 304 stainless steel, carbon in the form of grafoil, silicon, tungsten, and polytetrafluroethylene (Teflon®) and polyethylene plugs. Silicon and tungsten were removed at 6 times the rate of carbon; stainless steel was unaffected. A CDE generated from O_2 and CF_4 was more effective than O_2/N_2H_2. CF_4 is chemically very inert, although it is a narcotic at high concentrations and has an affinity for certain polymers so that proper choice of seals is important. The products of the process are destroyed before reaching the vacuum pump, which uses Fomblin® oil. O-rings in contact with the reactive neutrals need to be made of a resistant material such as Calrez® or Chemraz®.

Because tungsten is as good a witness as silicon and is readily and cheaply available in the form of welding rods of the right size to fit into the stems, it was decided that W rods could be used as witnesses to determine whether or not active etching had reached far enough into the stem to clean the area to be pinch welded. Contaminated stems were sectioned, characterized, reassembled into tubes to simulate an intact stem and CDEed. In some cases tungsten rods with polished ends were inserted part way into tubes to act as witnesses. It is very easy to detect evidence by eye of the etching process, even on unpolished tungsten (Figure 12).

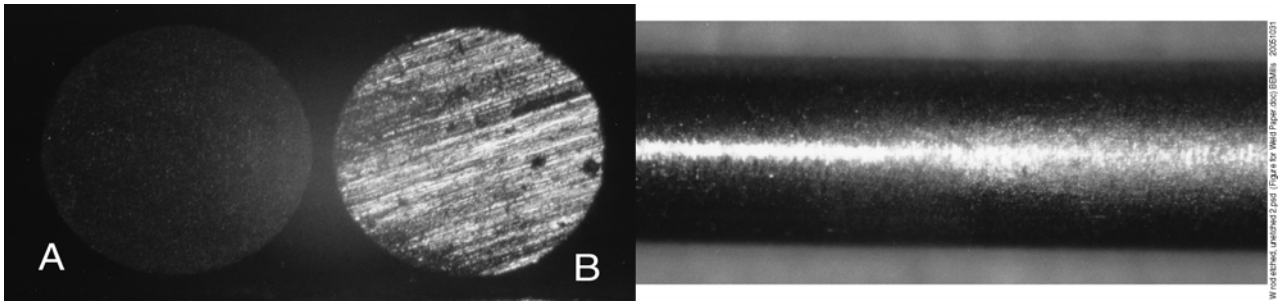

Figure 12. Tungsten rods used as a witness to chemical downstream etching. At left rods are shown A, polished, and B, polished and etched. At right is an unpolished rod showing that the right portion, which has been etched is easily distinguished from the unetched left hand side.

If any of the reactive atoms or molecules reside on the surface for long enough, they have a chance of encountering and recombining with another active species. This is more likely on a surface than in the free state because there is a surface to accept their excess energy. The recombination rate on stainless steel is significantly higher than it is on quartz. Since we only need to clean the portion of the stem destined to be pinch welded, a quartz sleeve in the outer portion of the stem can minimize the time necessary to clean the area of interest. Unfortunately this sleeve requires that the tungsten witness rod be inserted first and that would impede the pumping of the bottle. On the other hand the propensity of the reactive species to recombine on the steel surface means that the penetration of these species into the bottle is limited by the length of stem exposed inside of the weld area.

A tool was constructed specifically to clean stems (Figure 13) operating at 360 millitorr using a 13.56 MHz radio frequency plasma generator operating at 400 W. A 2" quartz tube contains, transports, and neutralizes the plasma while mass flow controllers meter in the oxygen at 160 and CF_4 at 60 sccm. Cleaning the parts takes 8 to 12 hours depending on the configuration and the material.

Figure 13. Custom chemical downstream etching (CDE) tool built to clean carbon-contaminated stems. Left: Tool, including control and pumping. Center: fixture to allow three bottles to be cleaned simultaneously. These bottles can be fitted with instrumentation to measure pressures and temperatures during development. Right: Tool with the power on showing the plasma.

Figure 14 shows SEM and carbon Auger maps of the same area before and after cleaning. Although the carbon has been removed, it is still possible to see the areas where it had been. Partly this is because the texture developed during the etching process with nitric/Nitradd did not affect this area and, particularly in the most heavily contaminated stems, there is a ghost of chromium oxide left behind that is visible. To eliminate this residual material, these stems were cleaned with Oakite Ruststripper and rinsed, while the interior was protected with an inflatable angioplasty balloon. This process was very successful.

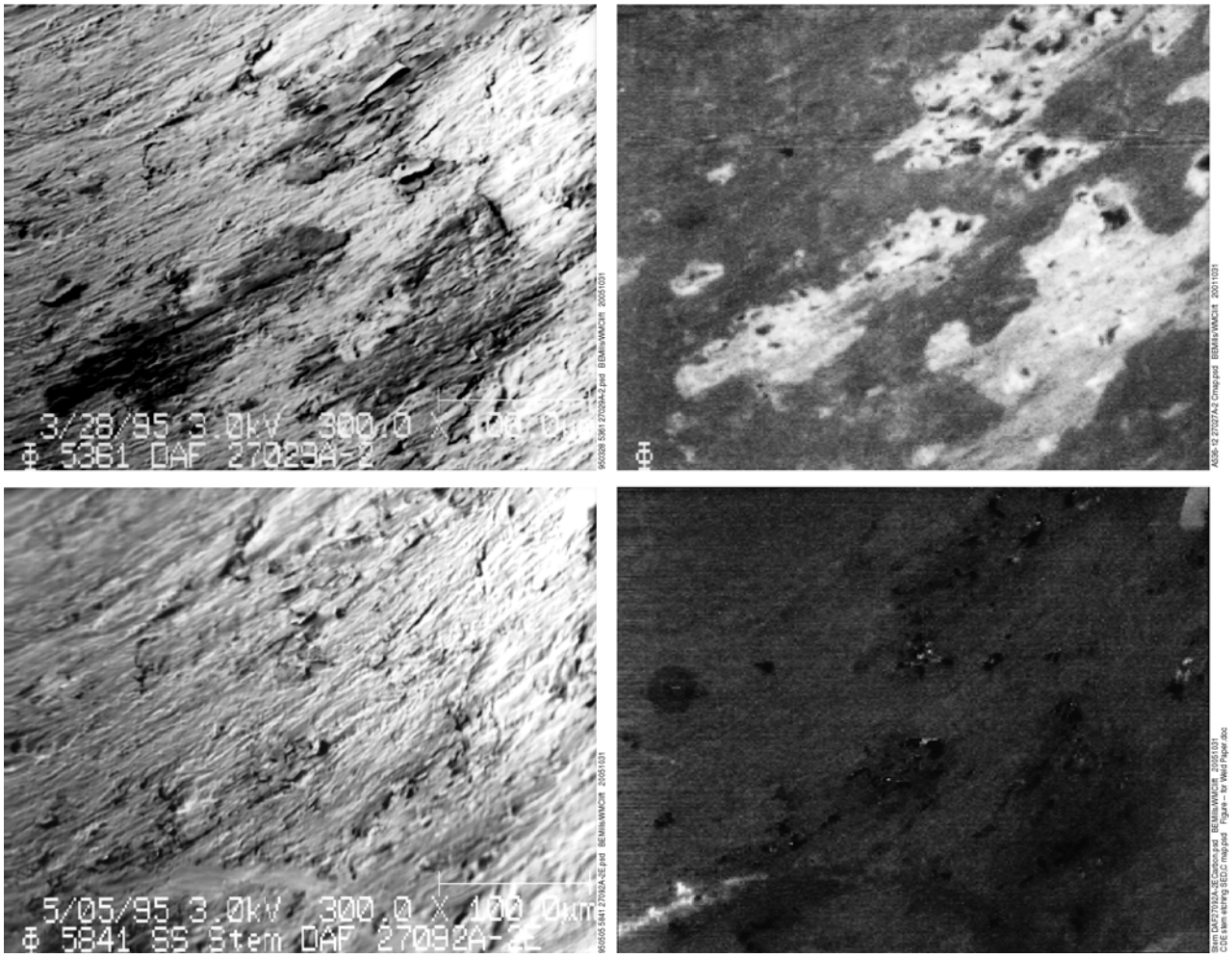

Figure 14. Interior of stem before (top) and after (bottom) chemical downstream etching. At left are secondary electron images (SEM) showing essentially the same area. At right are carbon Auger maps of the corresponding areas showing complete removal of the thick carbon deposits. The streak at the bottom left of the "after" images appears to be a handling artifact. The texture of the material under the carbon deposits does not appear etched because it was protected from the original nitric/Nitradd cleaning process.

Another technique that was considered for oxide removal was an ozone generator. [16] Ozone and ultraviolet light treatments can be effective in removing polymers because they cause depolymerization of the contaminant. That is not as effective on graphite. Carbon removal in a Tokamak has proved very difficult to perform. Even high energy helium/oxygen glow

discharges tend to only remove carbon in line-of-sight along the field lines. They are not effective in cracks between tiles and surfaces can be shadowed by microscopic impurities. The small amount of included chromium oxide that does not prevent cleaning by oxygen/carbon tetrafluoride CDE would stop glow discharge cleaning even if it penetrated into the stem.

Attempts at detecting contamination after welding

Ultrasonics had been attempted before [17] and is being attempted now at Kansas City Plant. In the earlier study samples of JBK 75 and HP 9-4-20 were vapor coated with 10-20 μ of silver and welded either at temperatures ranging from 110 to 400°C or in the range of 650-700°C at pressures up to 200 MPa (30 ksi). The former condition produced class 3-4 bonds (basically, non-bonding probably due to lack of flatness) and the latter condition produced class 1 welds. By doing 5 ultrasonic measurements per sample and using 4 of them as training samples, they were able to, in the JBK case 86% of the time and in the HP 9-4-20 case 100% of the time, predict the difference between a class 1 and a class 4 bond. The R-F spectra (Fourier Transform) of the reflected waveforms showed that only at the highest frequency, above 15 MHz, is it possible to distinguish class 1 and class 4 welds.

These results is consistent with work done in the mid 1990s by this author in conjunction with Merlin Micheal and the staff at SRS. At that time the Sandia, California ultrasonic inspection system was used on some preliminary cold welds, which showed promise. The equipment was then shipped to SRS and set up in the tritium building to look at the parts of interest. A 90 MHz transducer was used to get the best imaging. One problem with ultrasonics is that to see very small features, it is necessary to use a high frequency, but high frequency sound does not penetrate well. Another problem is that to be able to use the system it is often necessary to "train" the equipment with a large number of examples which are then classified by destructive inspection. In this case the contaminated welds were still quite good solid state welds and so gave little signal. In addition to that, there were very few welds available and each one had to be laboriously decontaminated before ultrasonics could be performed. Finally, it would have been necessary to sacrifice a number of good parts to confirm any observations from the ultrasonics. Ultimately there was not enough evidence of the effectiveness of ultrasonics or need to justify the sacrifice.

At the same time as the ultrasonic work was being done, the limited number of welds available for study were also inspected using a microfocus x-ray tube and using neutron radiography. The x-radiography did not detect any signal not accounted for by variation in weld thickness. If there had been a sufficient number of protons included with the graphite, the neutron radiography would have been able to detect them. Carbon can contain up to about 30% hydrogen. The cross-section for tritium and deuterium is quite small compared with that of protium. Of course, the imaging would have to be soon after production of the weld in tritium because of the very large cross-section of helium-3. This was not possible for units that had been filled some time ago. Therefore the neutron radiography did not yield useful results.

With the number of welds available it was not possible to determine a technique to asses their contamination nondestructively as a supplement to the physical and x-ray measurements already made.

Recommended future directions

For typical contaminants such as organics, oxides, and salts, we should restore our capability to perform reflection Fourier transform infrared (FTIR) spectroscopy on tubes and determine if it can be extended to inspect tubes open at only one end. This latter could be done using the natural emission from the surface that is heated to about 100°C (although a higher temperature would be better if permitted). This can be done in an inert atmosphere to minimize oxidation. We should determine if this tool can evaluate tubes stems contaminated with graphite and, if samples become available, the graphite/chromium oxide compound seen in the past.

For surfaces that will be subjected to inertia welding, the most promising specific tool is diffuse reflectance infrared (DRIFT) spectroscopy. It should be able to detect organic, oxide, and salt contamination. Its advantage over the OPO imaging method is that one spectrum can be expected to detect any of the above-mentioned contaminants, whereas OPO would have to image specific wavelengths for each type of contaminant. It could be that multivariate statistical analysis of the spectra would be needed, particularly if this were to become a routine post-cleaning pre-weld acceptance tool.

Although it is not recommended, if this type of oil is used again in this application it is possible to monitor its degradation by several methods. Discussed above are Fourier transform infrared spectroscopy (FTIR), thermogravimetric analysis (TGA), and size exclusion chromatography (SEC). Although all of these detect changes in the oil, the most specific tool would be FTIR as it distinguishes specific chemical changes. TGA is probably the easiest to interpret quantitatively and it measures an important property since one of the functions of the oil is to cool the part and for that it must remain liquid during use. If one were to characterize the oil in the future, liquid chromatography (LC) and gas chromatography (GC) coupled with mass spectroscopy (MS) could be useful. If formation of acid species are suspected (for example carboxylic acids), ion chromatography would be of interest. More specific signatures of oil breakdown can be isolated from this data, giving us a better picture of the mechanism for the loss of function seen in the TGA. Presumably these products could not be correlated with deposits of carbon/chromium oxide inside the tubes because the oil would be changed before its properties deteriorated to the point of producing the hot spots that would be associated with the deposits.

Despite efforts to avoid contamination, weld process data should be continue to be recorded and it should be archived so that any anomalies observed in future surveillance can be tied to a particular observable phenomenon if possible. Not all contamination shows up in this data, but some does.

Finally, with the purchase of a new nanofocus x-ray tube, our ability to image small parts such as pinch welds has improved by approximately an order of magnitude since the original work. If the problem of representative contaminated welds for study can be surmounted, imaging the interface should again be attempted.

This page intentionally left blank.

References

1. J. Spingarn and C. Lunbom, Pinch Weld, 304L Stainless Steel, Microstructure Standard, Sandia National Laboratories specification SB452907-000 Issue B, August 17, 1984.

2. W. Miles Clift, secondary and Auger electron images, spectra and depth profiles, presented at "Stem Contamination and Remediation Project, Anton J. West, June 6, 1995.

3. Tom Zifer, Oil Analysis by Size Exclusion Chromatography, Sandia National Laboratories memorandum to Pete Royval, June 2, 1995.

4. Statement by William R. Even, materials scientist, in e-mail, October 18, 2005.

5. Laboratory Notebook of Marion Hunter, technologist, October 5, 1995.

6. Roger G. Miller and David J. Stephan, *Pinch Weld Contamination Studies*, MLM-MC-90-31-0002-Redacted. Mound report available at Sandia National Laboratories Central Technical Files, Livermore, CA, original report issued November 9, 1990.

7. J. L. Jellison, The Role of Surface Contaminants in the Solid-State Welding of Metals, in *Treatise on Clean Surface Technology*, K. L. Mittal, ed., vol. I, pp. 205-234. Plenum Press, New York, NY, 1987. and J. L. Jellison, *The Role of Surface Contamination in the Solid State Welding of Metals*, SAND83-0547J. Sandia National Laboratories, Albuquerque, NM, March 1983. and J. L. Jellison, Effect of Surface Contamination on Solid Phase Welding—an Overview, in *Surface Contamination*, K. L. Mittal, ed., vol. 2, pp. 899-923, Plenum Press, New York, NY, 1979.

8. P. S. Korinko, S. H. Malene, G. J. McKinney, and W. D. Thonpson, *Pinch Weld Characterization of Particulate Contaminated Stems*, WSRC-TR-2004-00574. Westinghouse Savannah River Company, Aiken, SC, November 17, 2004.

9. R. W. Bradshaw, D. K. Ottesen, L. R. Thorne, A. L. Newman, and L. N. Tallerico, *Spectroscopic Characterization and Pinch Welding of Contaminated Tubing*, SAND87-8541. Sandia National Laboratories, Livermore, CA (OUO), December 1987.

10. D. K. Ottesen, L. R. Thorne, and R. W. Bradshaw, *The Detection of Contaminants in Narrow-Bore Tubing by Infrared Relfection Spectroscopy*, SAND86-8789. Sandia National Laboratories, Livermore, CA, June 1986.

11. David Ottesen, Howard Johnsen, Sarah Allendorf, Tom Kulp, Karla Armstrong, Scott Robinson, Peter Ludowise, and Uta Goehrs, *Detection of Surface Contaminant Residue By Tunable Infrared Laser Imaging*, SAND2001-8262. Sandia National Laboratories, Livermore, CA, June 2001. and P. D. Ludowise, J. S. Robinson, D. K. Ottesen, T. J. Kulp, U. B. Goers, K. Armstrong, and S. W. Allendorf, A Laser-Based System for Chemical Imaging, in *OSA Trends in Optics and Photonics*, vol. 36, pp. 160-162, 2000.

12. G. Louis Powell, Tye E. Barber, John T. Neu, and Billy H. Nerren, Diffuse Reflection Mid-Infrared Spectroscopy as a Tool for the Identification of Surface Contamination on Sandblasted Metals, in *Second Aerospace Environmental Technology Conference*, held in Huntsville, AL, August 6-8, 1996. NASA Conference Publication 3349, A. F. Whitaker, M. Clark-Ingram, and S. L. Hessler, eds., March 1997. and George L. Powell, Tye E. Barber, Mariza Marrero-Rivera, David M. Williams, Norma R. Smyrl, and John Neu, Oil Anylysis

on Metal Surfaces by Using DR-FT-IR Mapping Techniques, in *Mikrochim. Acta [Suppl.]*, vol. 14, pp. 655-656, 1997.

13. Alfred A. Christy, Yukihiro Ozaki, and Vasilis G. Gregoriou, *Modern Fourier Transform Infrared Spectroscopy*, vol. XXXV of *Comprehensive Analytical Chemistry*, ed. D. Barceló, Elsevier, New York, NY, 2001.

14. M. G. Benkovich and J. L. Anderson, A New Method Using MESERAN Technique for Measuring Surface Contamination after Solvent Extraction, at *International Symposium on Surface Contamination and Cleaning*, held in Newark, NJ, May 23-25, 2001, published in *Surface Contamination and Cleaning*, vol. 1, pp. 49-73, 2003.

15. Tuan Vo-Dinh, Characterization of Surface Contaminants by Luminescence Using Ultraviolet Excitation, in *Treatise on Clean Surface Technology*, K. L. Mittal, ed., vol. 1, pp. 103-122. Plenum Press, New York, NY, 1987.

16. John R. Vig, UV/Ozone Cleaning of Surfaces: A Review, in *Surface Contamination*, K. L. Mittal, ed., vol. 1, pp. 235-254. Plenum Press, New York, NY, 1979.

17. Graham Thomas and Jay Spingarn, Ultrasonic Non-Destructive Evaluation of Solid State Welds, in *Review of the Progress of Quantitative Non-Destructive Evaluation*, vol. 7B, pp. 1319-1325, 1988.

Appendix A

3.3.1 Melting

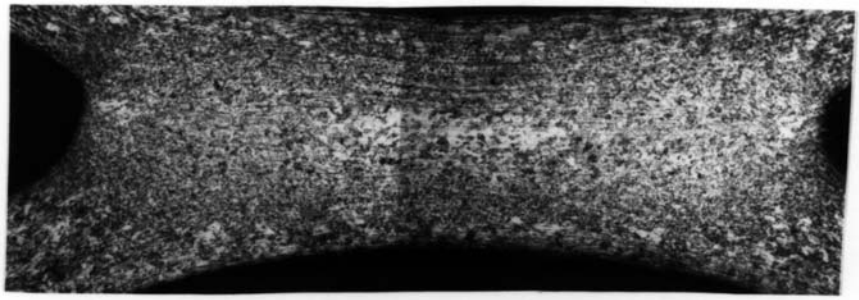

I. Solid State - No evidence of melting or grain boundary transformations.

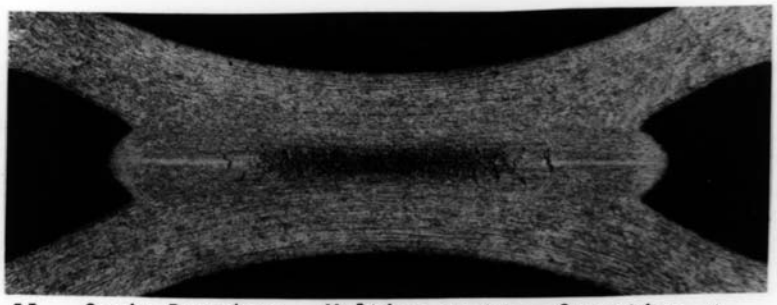

II. Grain Boundary - Melting or transformation at the grain boundaries.

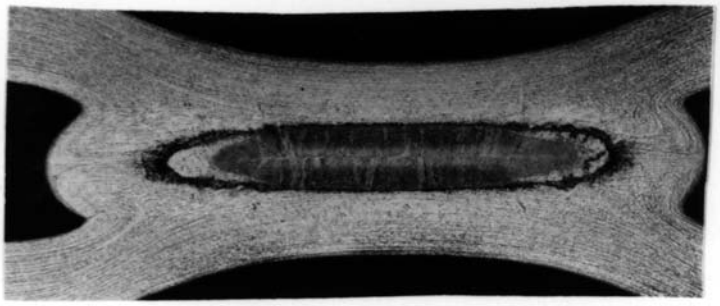

III. Melt Nugget - Melting and resolidification of the bulk metal.

FIGURE 1 - TYPICAL MACROSTRUCTURES OBSERVED IN PINCH WELDS. THESE PHOTOGRAPHS ARE TO BE USED TO RATE TYPE OF MELTING IN EITHER LONGITUDINAL OR TRANSVERSE METALLOGRAPHIC SECTIONS. ALTHOUGH THESE PHOTOMICROGRAPHS ARE TAKEN FROM CONFINED PINCH WELDS, THE GROSS APPEARANCE OF MELTING IN UNCONFINED PINCH WELDS WILL BE SIMILAR.

3.3.2 Bond Line

Class 1. Interface not visible in etched condition. Good grain growth across entire length of interface.

FIGURE 2 - STANDARD PHOTOMICROGRAPHS (500X) FOR EVALUATING PINCH WELD BOND QUALITY FOR SPECIMENS ETCHED USING ELECTROLYTIC OXALIC ACID.

FIGURE 2 Continued.

Class 2. Remmants of interface visible but discontinuous. Grain growth or recrystallization along entire length of bond. Some contaminants visible.

FIGURE 2 - STANDARD PHOTOMICROGRAPHS (500X) FOR EVALUATING PINCH WELD BOND QUALITY FOR SPECIMENS ETCHED USING ELECTROLYTIC OXALIC ACID.

FIGURE 2 Continued

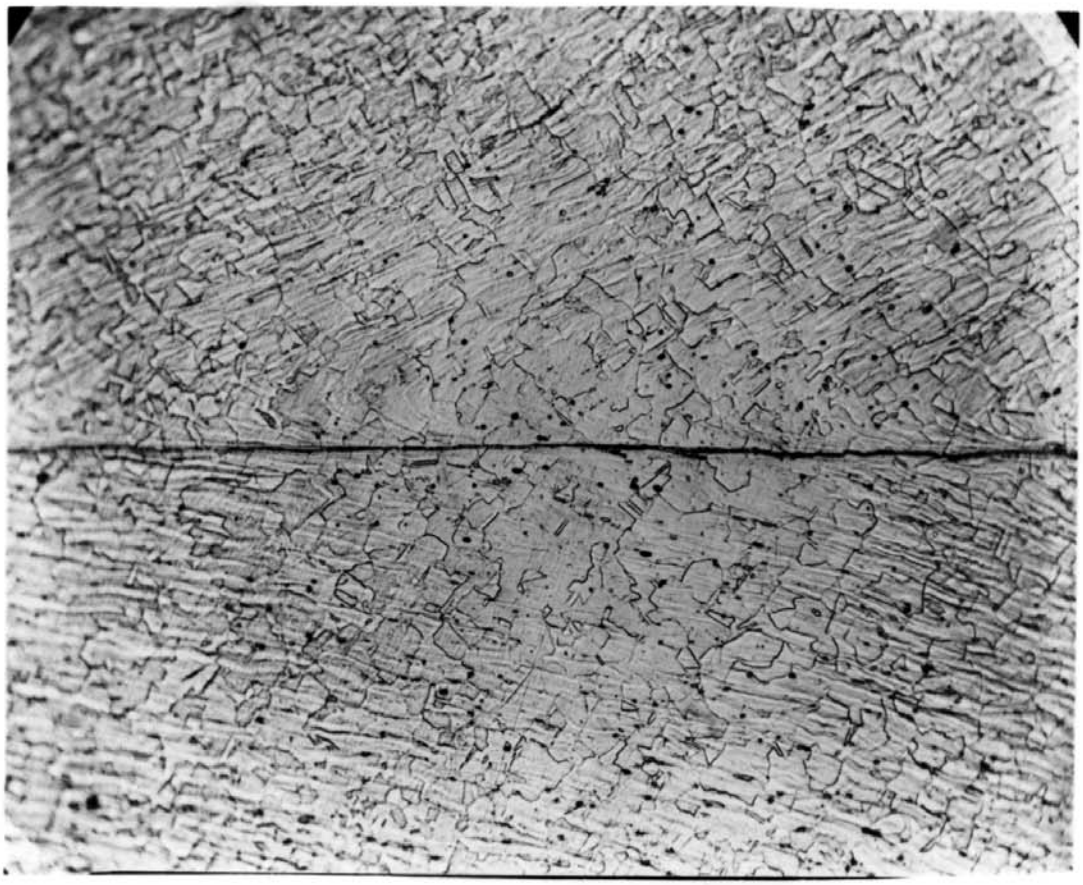

Class 3. Interface may be faintly visible in unetched condition and almost continuous in etched condition. Recrystallization or grain growth along interface.

FIGURE 2 - STANDARD PHOTOMICROGRAPHS (500X) FOR EVALUATING PINCH WELD BOND QUALITY FOR SPECIMENS ETCHED USING ELECTROLYTIC OXALIC ACID.

FIGURE 2 Continued

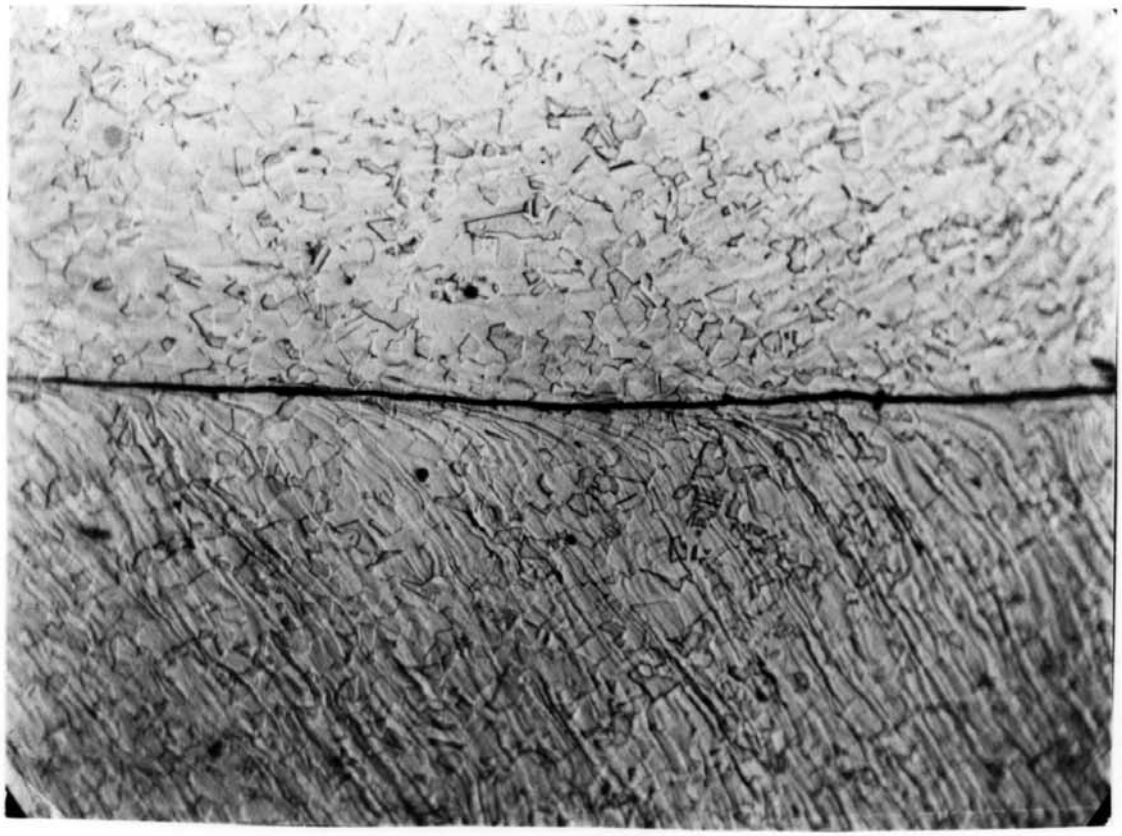

Class 4. Interface clearly visible in unetched condition. No grain growth; residual cold work remains. Gross contamination.

FIGURE 2 - STANDARD PHOTOMICROGRAPHS (500X) FOR EVALUATING PINCH WELD BOND QUALITY FOR SPECIMENS ETCHED USING ELECTROLYTIC OXALIC ACID.

3.3.2 Bond Line (Continued)

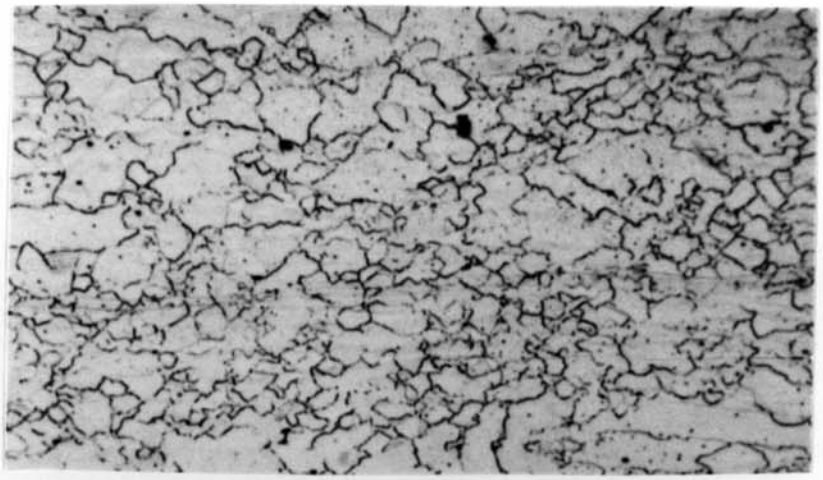

Class 1 - Interface not visible in etched condition. Good grain growth across entire length of interface.

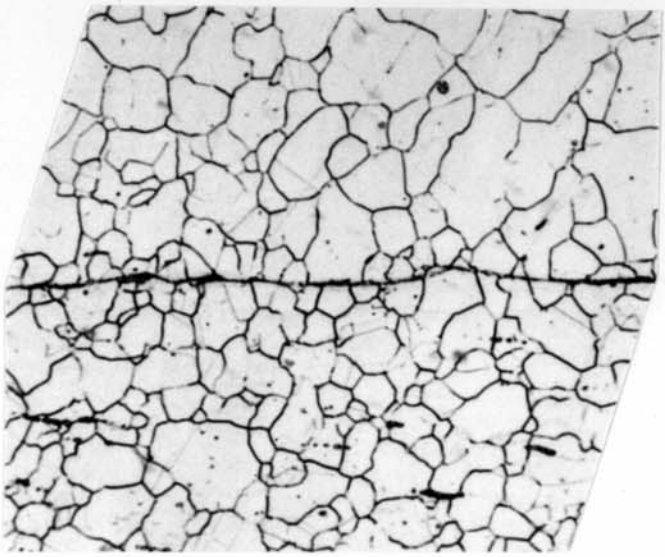

Class 2 - Remnants of interface visible, but shallow etch depth. Grain growth or recrystallization along entire bond. Some contaminants.

FIGURE 3 - STANDARD PHOTOMICROGRAPHS (500X) FOR EVALUATING PINCH WELD BOND QUALITY FOR SPECIMENS ETCHED USING ELECTROLYTIC NITRIC ACID.

FIGURE 3 (Continued)

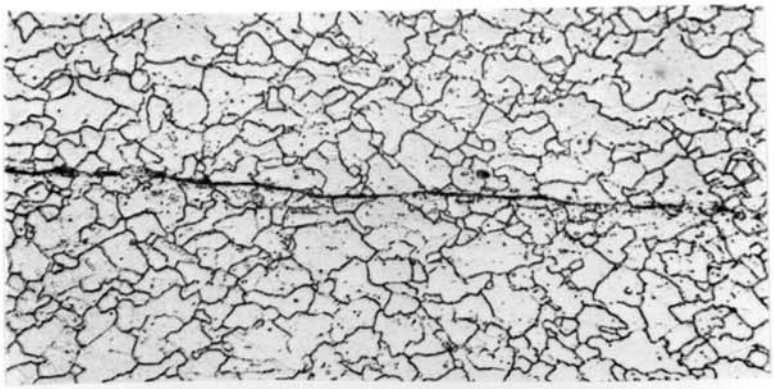

Class 3. Interface may be faintly visible in unetched condition and almost continuous in etched condition. Recrystallization or grain growth along interface.

FIGURE 4 - STANDARD PHOTOMICROGRAPHS (500X) FOR EVALUATING PINCH WELD BOND QUALITY FOR SPECIMENS ETCHED USING ELECTROLYTIC NITRIC ACID.

3.3.3 Defects

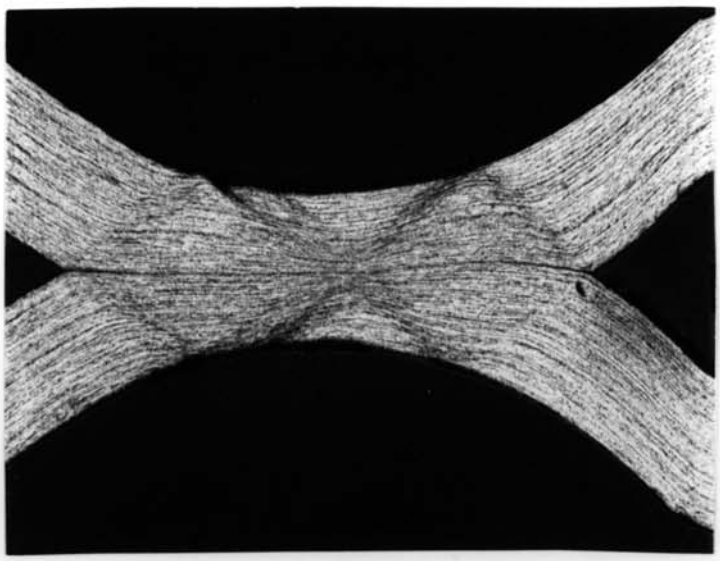

Shear Band - Sharp discontinuity in grain structure.

Spitting - Detached resolidified metal.

FIGURE 4 - TYPICAL DEFECTS OCCASIONALLY OBSERVED IN LONGITUDINAL SECTIONS OF PINCH WELDS (BOTH CONFINED AND UNCONFINED).

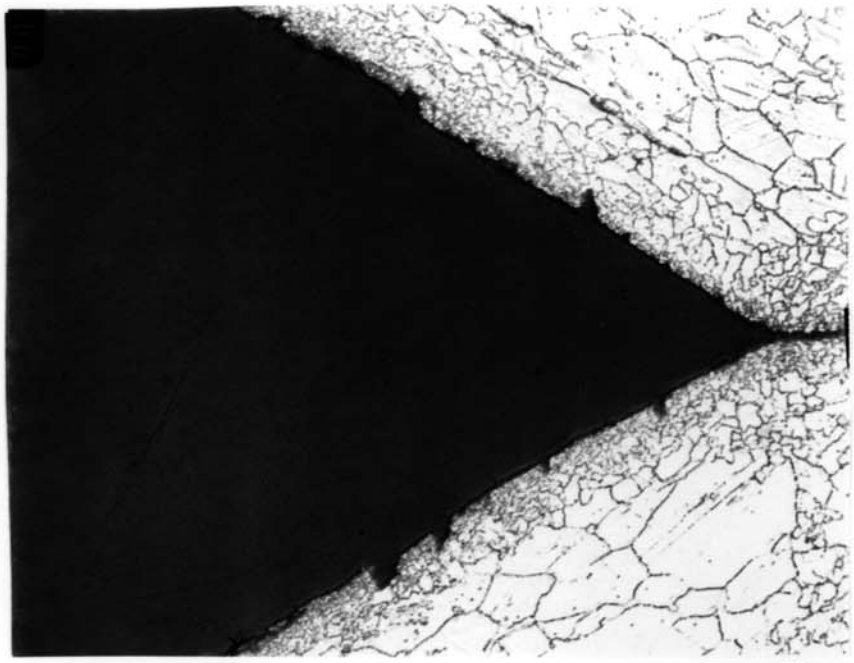

Micro-Cracking at
Inside Surface

Micro-Shear Bands at
Inside Surface

Figure 4 - TYPICAL DEFECTS OCCASIONALLY OBSERVED IN LONGITUDINAL SECTIONS OF PINCH WELDS (BOTH CONFINED AND UNCONFINED).

This page intentionally left blank.

Appendix B

ABSTRACT

A series of studies were conducted to determine the effect of various contaminants on the bond quality of pinch welds and the ability of data acquisition systems (DAS) to determine the presence of contaminants. Studies were conducted on confined pinch welds using 304L and 21-6-9 materials. A more limited study on unconfined pinch welds used 304L material. Bond quality measurements were made using SNL specification SS452907 and SB452907. Results indicate that some contaminants severely affect weld quality. Results also show data acquisition systems may be able to indicate that contaminants were present.

INTRODUCTION

Pinch welds (confined and unconfined) are used to seal reservoirs for gas boost systems. A high quality and repeatable process is required to seal the unit from the environment.

PINCH WELD EQUIPMENT

Equipment

The pinch weld equipment (Mound Drawing FSE199931) used for these studies was designed at Mound and is very similar to the New Program One pinch welders in use at SRS [1]. There are currently fourteen systems in use for production and development activities. The pinch welding system has previously been described in detail [2]. The other major components in the welding system include a Pertron PWC-300 weld controller, Pertron Silicon Controlled Rectifiers (SCRs), and a Kirkhof transformer.

Welding electrodes (Mound Drawing AYD860112 and AYD860805) used are of a standard design for pinch welding and are composed of an RWMA (Resistance Welders Manufacturer's Association) Class 2 shaft with an RWMA 13-tip having a cyclinderical radius of 3/32 or 3/16 in., depending on the application and program requirements.

Fixtures (Mound Drawing AYD860385 and AYD860116) used during the experiments enabled confined pinch welds to be made. Except for the material used to fabricate them, these fixtures are identical to those used in production and

development at SRS. At SRS the cited material is 17-4 PH stainless steel. This was changed to 316 stainless steel at Mound for two reasons. First, it is common practice to minimize the amount of ferromagnetic material in the secondary arm of the welding equipment. Second, the use of ferromagnetic materials in fixtures has been shown to induce voltages (noise) on the DAS monitoring the secondary weld voltage.

Data Acquisition System

The data acquisition system (DAS) used throughout the series of experiments is Mound's third generation of DAS for resistance welding. The system was developed in 1986 and is a computer-based system. The DAS is capable of:

- recording the secondary voltage waveform and calculating the RMS voltage,
- recording the secondary current waveform and calculating the RMS current,
- recording the force waveform and calculating the mean force, and
- recording the displacement waveform.

The system can also record individual displacements and primary voltage before and after welding. The computer system also controls a host of other equipment. Other important system functions that are controlled by the computer include controlling an electronic pressure regulator for the application of the welding force, downloading welding schedules to the Pertron weld controller, formatting and outputting welding data, instructing the welding operator, monitoring and controlling safety interlocks, and performing calibration routines.

EXPERIMENTAL DESIGN

CONTAMINATION MATRIX

Table 1 shows the contaminants that were studied and their possible source.

Table 1 - CONTAMINANTS AND POSSIBLE SOURCE

Contaminant	Possible Source
Copper Wire	Copper Gaskets
Oxide	Unetched Stems
Cotton Fiber	Gloves
Silicone Grease	Vacuum Systems
Polyethylene	Contamination Control Caps
WD-40	Light Oils
Nylon Bristles	Cleaning and Decon Brushes
EDM	EDM Tubing

Table 2 shows the welding conditions for the matrix. Factors include contaminant, atmosphere inside tubing during welding, weld type, and material type. The first seven contaminants were for both 304L and 21-6-9 materials.

Electrical discharge machined (EDM) stems of 304L were welded only as an unconfined pinch. Although the presence of some of the contaminants seemed unlikely, including them in the list provided for a wide variety of materials to be studied. Both organic and inorganic materials were included, and a wide variety of molecular weights for organic materials allowed for some general conclusions to be made at the end of the studies. A total of 45 welds were completed for the studies.

Table 2 - WELDING CONDITIONS

	Confined Pinch						Unconfined Pinch					
	Material Type						Material Type					
	304L			21-6-9			304L			21-6-9		
	Atmosphere			Atmosphere			Atmosphere			Atmosphere		
Contaminant	Ox	Red	Vac	Ox	Red	Vac	Ox	Red	Vac	Ox	Red	Vac
Copper Wire	X			X								
Oxidized	X			X								
Cotton Fiber	X			X								
Silicone	X			X								
Polyethylene	X			X								
WD-40	X			X								
Nylon Bristles	X			X								
EDM								X	X			

WELDING PROCEDURES

Three welding procedures were used to weld the various combinations of the studies. Table 3 shows the procedures used and some of the acceptance criteria. All welds were made on the same pinch welder to simplify comparisons. For the fourteen pinch welding systems in use at Mound, the procedures (heat setting and resulting current) vary from machine to machine in order to maximize the operating range of any particular piece of equipment.

Table 3 - WELDING PROCEDURES AND ACCEPTANCE CRITERIA
PINCH WELDER #13

Electrode Size (in)	Heat Percent		Current Limits (Kamp)		Welding Cycles		Welding Force (lbf)		Weld Thickness (in)		Weld Width (in)	
3/32	32	40	2.60	3.19	11	13	1050	1150	0.048	0.058	0.135 MAX	
3/32	39	50	3.15	3.90	6.5	7.5	775	825	0.026	0.042	0.165	0.200
3/16	47	55	3.50	4.15	11	13	1200	1300	0.050	0.060	0.135 MAX	

Welding procedures used in the studies for the confined pinch welds were chosen to produce a microstructure just on the verge of incipient melting at the center of the weld. It would then be possible to judge whether the contaminants might cause a nugget to be formed and, therefore, be more likely to cause cracking by maximizing the amount of contaminant in the small melted areas. A variety of heat conditions were used on unconfined welds to better evaluate the degradation in bond quality. Because of lower heat input and the inability to control large weld nuggets, unconfined pinch welds generally do not produce melting.

RESULTS

Pinch welds were examined in the normal manner. Data acquisition was recorded, physical measurements taken, proof-testing, radiography, and metallurgical evaluations were conducted on the test stems.

Confined and unconfined welds on 304L all passed a 40,000 psi hydrostatic proof test. Confined welds on 21-6-9 were proofed at pressures greater than 70,000 psi. Again all welds passed proof-testing. Radiography was unable to detect defects in the bond line or the small amount of extrusion cracking with copper contamination. Metallurgical cross-sections were taken in the longitudinal and transverse directions.

DATA ACQUISITION

Data acquisition data were analyzed to determine whether the DAS could detect the presence of contaminants. Two possible resulting actions of the DAS would either inform the welding operator after the weld was completed or possibly modify the welding procedure during the weld. Tables 4-6 show data acquisition results that were compared for the three weld types. Stems without contamination (standards) were processed along with contaminated stems for comparison purposes. The weld cycles and force were held constant at the nominal setting for all welds. The heat setting was also held constant, except for welds examining the EDM tubing and the metal particulate contamination.

Secondary current, secondary voltage, weld displacement, rate of weld displacement, and weld resistance (preweld and during) were compared.

Table 4 - DATA ACQUISITION RESULTS FOR UNCONFINED PINCH WELD ON 304L

Weld	Contaminant	Heat Setting	Weld Current (KAmp)	Weld Voltage (Volts)	Preweld Resistance (Ohm)	Weld Displacement (In)	Weld Thickness (In)
158803	Standard	53	3.95	0.80	0.0016	0.045	0.021
648503	Standard	43	3.39	0.78	0.0012	0.031	0.035
648501	Standard	37	3.01	0.73	0.0014	0.021	0.042
20001	EDM	53	3.99	0.79	0.0011	0.039	0.023
20002	EDM	53	3.99	0.79	0.0010	0.042	0.021
30001	EDM	43	3.30	0.77	0.0011	0.030	0.035
30002	EDM	43	3.37	0.77	0.0013	0.028	0.035
40001	EDM	37	3.04	0.70	0.0012	0.019	0.041
40002	EDM	37	3.01	0.73	0.0010	0.022	0.042

Table 5 - DATA ACQUISITION RESULTS FOR CONFINED PINCH WELDS ON 304L

Weld	Contaminant	Heat Setting	Weld Current (KAmp)	Weld Voltage (Volts)	Preweld Resistance (Ohm)	Weld Displacement (In)	Weld Thickness (In)
5232	Standard	51	3.80	0.82	0.0053	0.027	0.054
6071	Copper Wire	51	3.57	0.83	0.0053	0.026	0.054
6072	Copper Wire	51	3.65	0.82	0.0027	0.025	0.056
9131	Copper Wire	51	3.88	0.81	0.0034	0.026	0.056
9150	Oxidized	51	3.85	0.87	0.0450	0.027	0.055
9151	Oxidized	51	3.84	0.90	0.0780	0.027	0.054
9152	Oxidized	51	3.86	0.85	0.0570	0.023	0.053
9132	Nylon	51	3.89	0.81	0.0010	0.025	0.052
9133	Nylon	51	3.62	0.82	0.0020	0.024	0.054
9134	Nylon	51	3.60	0.81	0.0020	0.025	0.055
9135	Cotton Fiber	51	3.91	0.81	0.0020	0.024	0.055
9136	Cotton Fiber	51	3.63	0.81	0.0020	0.025	0.055
9137	Cotton Fiber	51	3.89	0.81	0.0020	0.025	0.055
9138	Polyethylene	51	3.61	0.81	0.0027	0.024	0.055
9139	Polyethylene	51	3.62	0.82	0.0039	0.024	0.055
9140	Polyethylene	51	3.61	0.81	0.0038	0.024	0.055
9142	Silicone	51	3.90	0.82	0.0039	0.025	0.055
9144	Silicone	51	3.81	0.82	0.0033	0.025	0.055
9147	Silicone	51	3.89	0.82	0.0022	0.025	0.055
9148	WD-40	51	3.90	0.82	0.0025	0.025	0.056
9149	WD-40	51	3.90	0.83	0.0035	0.027	0.055
9154	WD-40	51	3.89	0.82	0.0024	0.024	0.056

Table 6 - DATA ACQUISITION RESULTS FOR CONFINED PINCH WELD ON 21-6-9

Weld	Contaminant	Heat Setting	Weld Current (KAmp)	Weld Voltage (Volts)	Preweld Resistance (Ohm)	Weld Displacement (In)	Weld Thickness (In)
2503	Standard	36	2.92	0.77	0.0054	0.031	0.052
7578	Copper Wire	36	2.91	0.78	0.0510	0.032	0.050
7579	Cotton Fiber	36	2.79	0.78	0.0190	0.033	0.051
7580	Polyethylene	36	2.92	0.78	0.0290	0.033	0.050
7581	Nylon	36	2.92	0.78	0.0290	0.033	0.050
7582	WD-40	36	2.70	0.78	0.0250	0.031	0.050
7583	Silicone	36	2.93	0.77	0.0230	0.032	0.049
7584	Oxidized	36	2.84	0.89	0.0910	0.033	0.047

SECONDARY WELD CURRENT

Examination of the data indicated that some differences between clean and dirty stems were detectable. Secondary weld current variations were much greater than normal. Under normal welding conditions, a series of welds made in a short time (one to several days), have shown a current variation range as little as 10 to 20 A. Over a longer timespan of months or a year the variation in current will be only slightly greater than the calibration error (2.5% of the reading). In these studies, current variations were as high as several hundred amperes for copper, nylon, and cotton fiber contamination. In a production environment, current variations of this magnitude would have indicated that an out-of-control situation was occurring.

SECONDARY WELD VOLTAGE

Evaluation of the secondary weld voltage indicated that only the oxidized stems showed significant variations. The increase in voltage drop through the weld can be explained by the increased resistance at the weld interface. Figure 1 shows the peak weld voltage as a function of weld cycle for a cleaned stem and several contaminated stems.

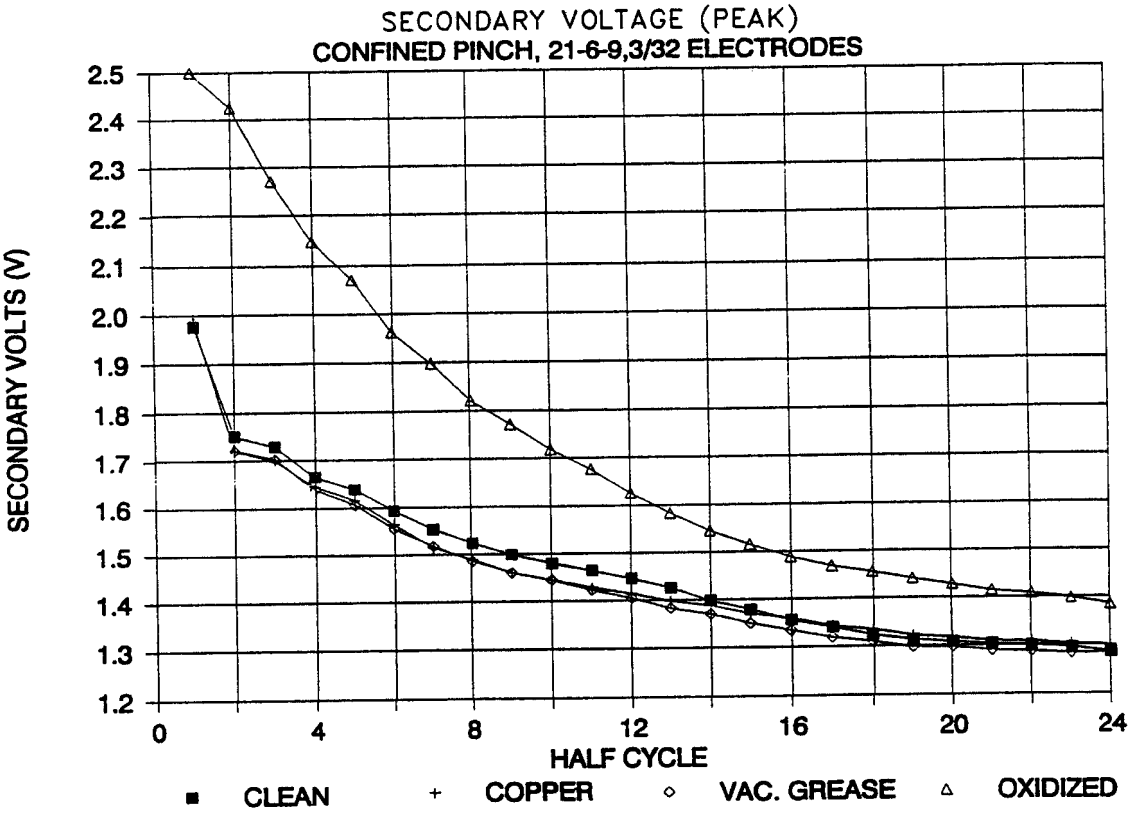

Figure 1 - Secondary weld voltage as a function of weld time.

WELD DISPLACEMENT

Weld displacement (as shown in Tables 4-6) is the total amount of displacement that occurs during the weld and does not include the amount of displacement during the squeeze cycle (cold pinch) prior to current flow. Weld displacement data did not indicate large differences between clean and contaminated stems. This may be partly explained by calibration error. Displacement transducers at Mound have an uncertainty of 0.002 in. A more accurate measurement, allowing for contamination, is final weld thickness. Final weld thickness for confined pinch welds on 21-6-9 showed a thinner weld when stems had been contaminated. The most thinning occurred with the oxidized tube (approximately 0.005 in. with respect to the standard tube).

RATE OF WELD DISPLACEMENT

Figure 2 shows the cumulative displacement as it takes place during a weld for a clean stem and stems contaminated with cotton fiber and heavy oxide. Note that there is little difference between the shape of the displacement curves. The oxide trace consistently remains above the other curves because the oxidized tube became thinner during welding.

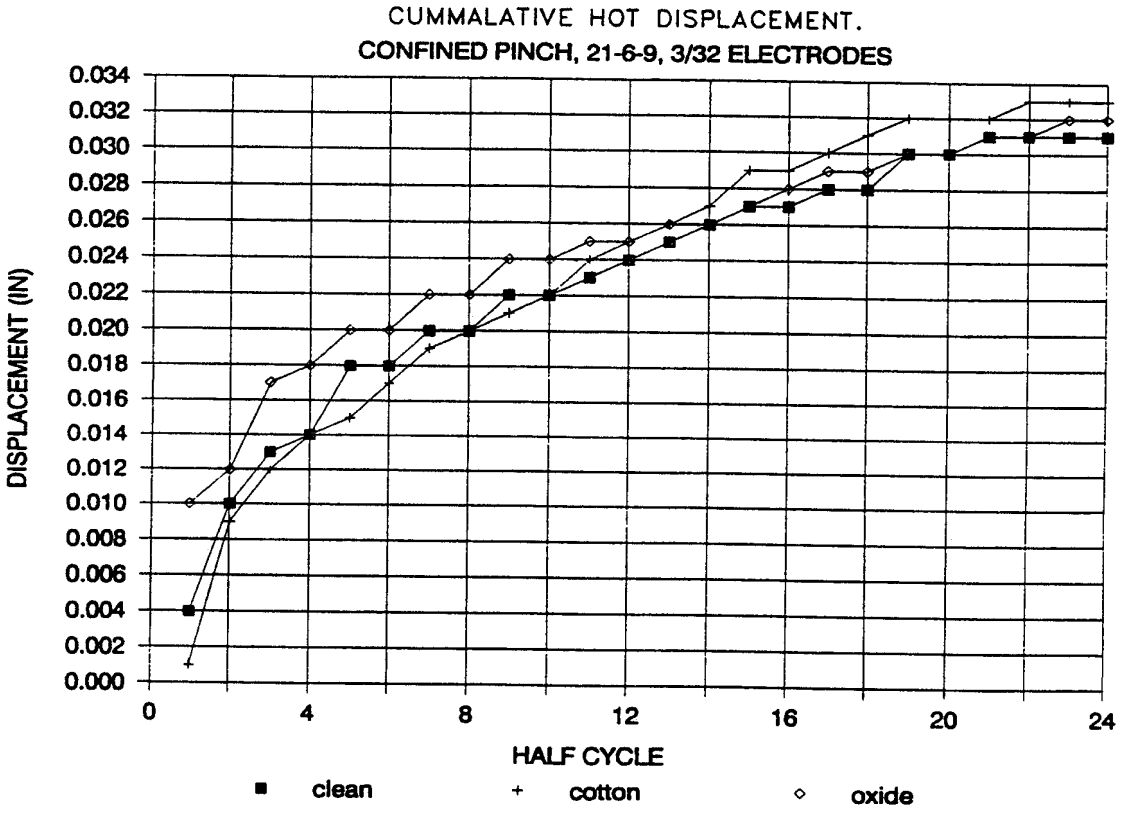

Figure 2 - Weld displacement as a function of weld time.

WELD RESISTANCE

At Mound and SRS, a preweld resistance check is made to determine whether there is contamination of the weld stem and to confirm that the welding electrodes are in adequate contact with the stem and that there are no major deficiencies in the current path. Other variables that affect preweld resistance are the cleanliness of the electrodes and the outside of the weld stem.

Preweld resistance is determined by passing a very low current through the stem during the squeeze cycle and measuring the voltage drop across the electrodes. A maximum value of 0.05 Ω has generally been the value used. In these studies, only oxidized stems consistently produced high preweld resistance. Copper contamination in the case of 21-6-9 also produced high preweld resistance.

Weld resistance during the weld was obtained by calculating a value using the peak current and voltage for each half cycle. Figure 3 displays the values

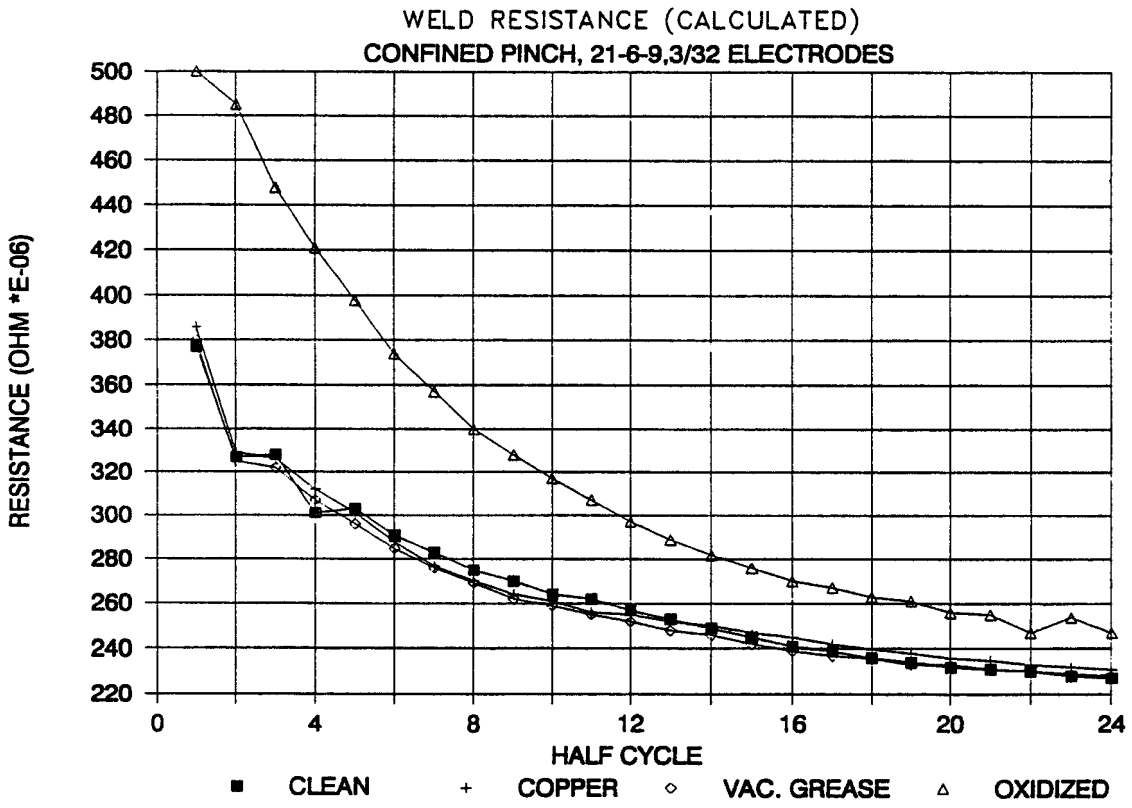

Figure 3 - Weld resistance as a function of weld time.

obtained for a clean stem and for a stem with various contaminates. Only in the case of the oxidized tubing is there a dramatic difference in resistance during welding. This figure is very similiar to Figure 1, as current variations from cycle to cycle are miminal.

The weld controller (Pertron PWC-300) provides constant current from cycle to cycle by monitoring the primary voltage and adjusting the firing angle of the SCRs as necessary during the weld. The controller is able to compensate for a positive or negative fluctuationn in primary voltage. In normal processing at Mound, production welding allows for deviations from nominal of up to 20 V.

Metallurgy

Metallurgical cross-sections were taken in the longitudinal manner for unconfined welds on 304L and confined welds on 21-6-9. Cross-sections were taken in longitudinal and transverse directions for confined pinch welds on 304L. All welds were evaluated per SNL specification SB452907 and SS452907 [3,4].

The samples were prepared in the usual manner. They were etched with electrolytic nitric acid (50% Nitric - 50% H_2O) following a pre-etch with a special mixture of nitric acid, hydrochloric acid, acetic acid, and glycol.

To maintain consistency and clarity, only the photographs of the longitudinal sections are presented in this report. (To present all of the welds sectioned would entail several hundred photographs.) The following sections will present only a select number of the welds but provides the flavor of the weld quality due to various contaminants.

STANDARDS

Figures 4-6 show a typical section of an unconfined pinch weld on 304L. This weld was produced at the minimum heat conditions with an atmosphere of 35 psi hydrogen inside the tube during welding. As seen in the figures, this weld has a bond quality rating of "1." This is evidenced by the complete lack of a prior interface in the etched condition.

Figures 7-9 are sections of confined pinch weld on 304L. These figures are also representative of the 21-6-9 material standard. (These are not

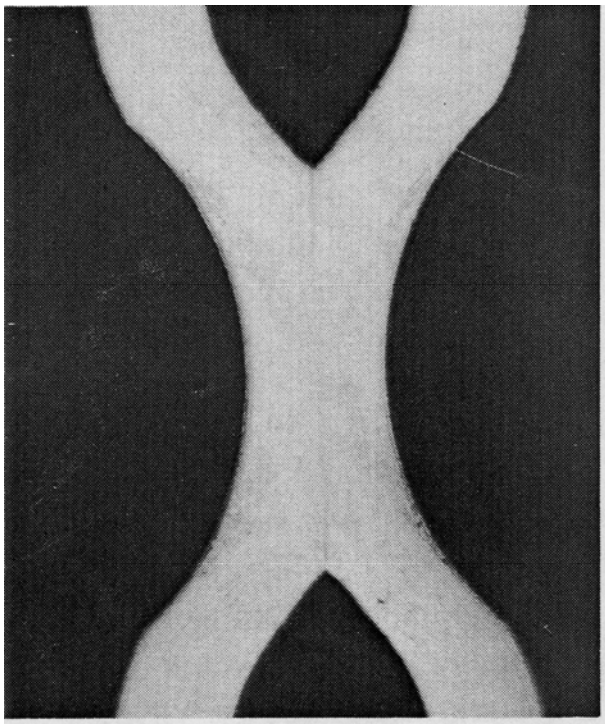

Figure 4 - SN 648501, standard pinch 304L. (22X)

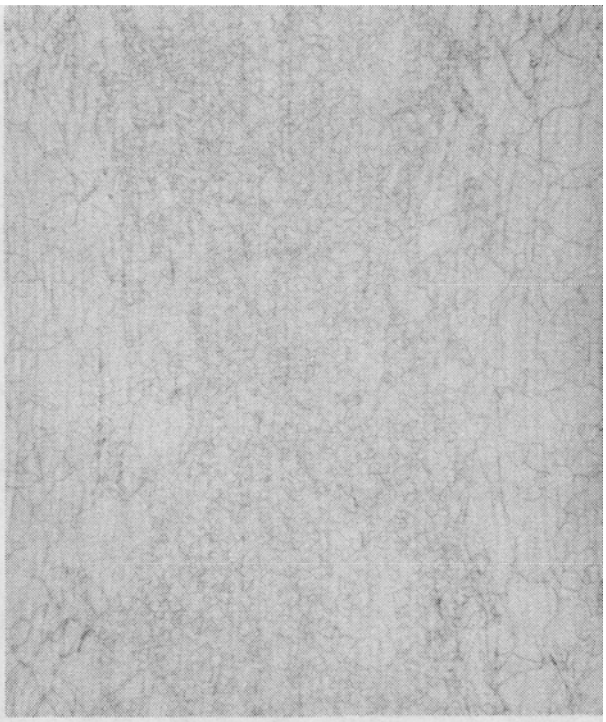

Figure 5 - SN 648502, standard pinch 304L. (100X)

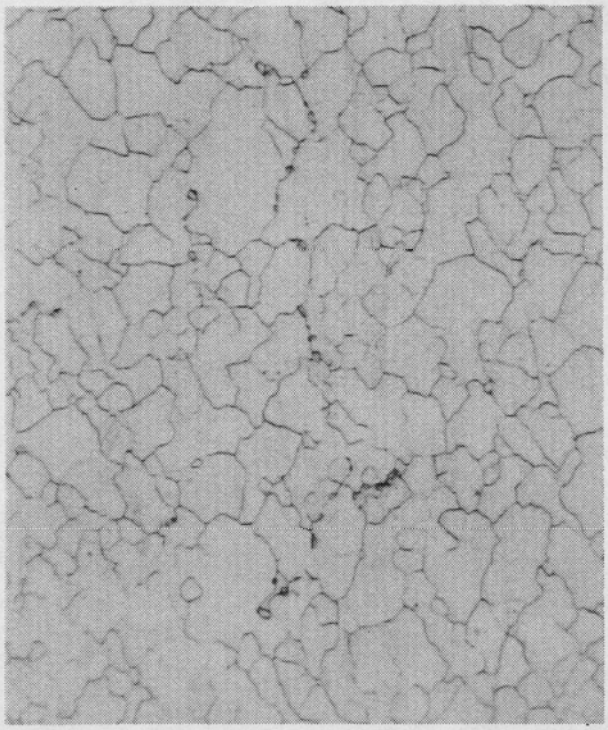

Figure 6 - SN 648501, standard pinch 304L. (500X)

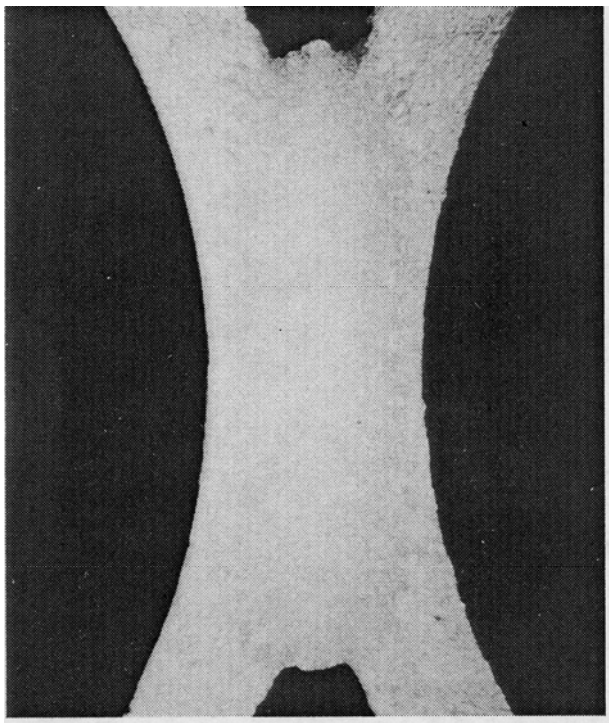

Figure 7 - SN 5232, confined pinch 304L. (22X)

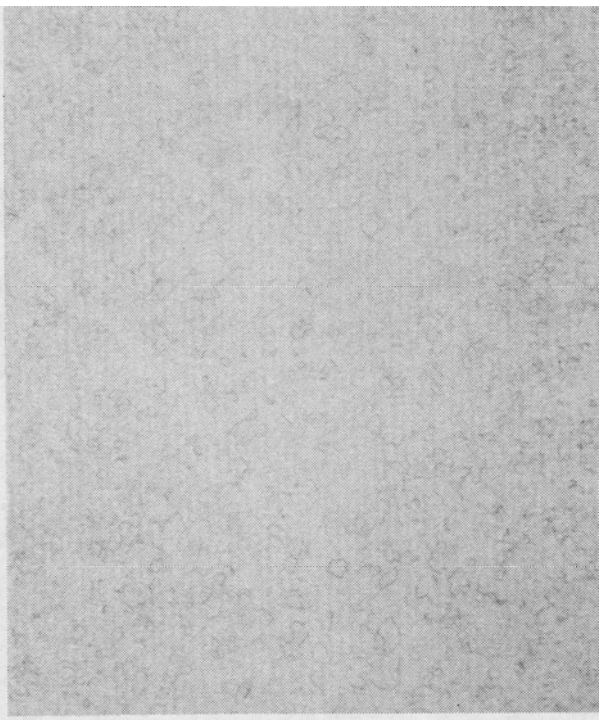

Figure 8 - SN 5232, confined pinch 304L. (100X)

Figure 9 - SN 5232, confined pinch 304L. (500X)

representative of cases in which 3/32-in. electrodes are used for 21-6-9, resulting in a shorter closure length.) The weld in Figures 7-9 was produced at nominal welding conditions with air being the atmosphere inside the stem. As with the unconfined pinch weld, the bond quality is excellent. In an air atmosphere, confined welds are able to produce a higher bond quality than unconfined pinch welds because of the higher heat input, longer weld times, and greater metal movement caused by lateral restraint of the weld by the confinement anvils.

CONTAMINANT: WD-40

As can be seen in Figures 10-13, WD-40 had little effect on the bond quality of confined welds on 304L or 21-6-9. Note that for 21-6-9, a small amount of incipient melting starts to occur. This feature was repeated throughout the studies. It is likely that this is caused by a slightly greater interface resistance caused by contamination.

CONTAMINANT: COTTON FIBER

Cotton fiber caused large variations in bond quality. Figures 14 and 15 show the effect of cotton fiber on 304L. The bond line has significant grain growth across the interface. The main defect is the numerous etch pits along the prior interface. Figures 16-18 show the effect on welding 21-6-9 material. Here a double or triple bond line is formed and a moderate amount of grain boundary melting occurs in the center of the weld. Even with this extremely poor bond, this weld passed a proof test of 80,400 psi.

CONTAMINANT: COPPER

The effect of copper contamination when welding stainless steel is well known. Examination of pinch welds with copper contamination indicated cracking only in the extrusion area. It may be that the electrode force in the center weld area is able to prevent the cracks from opening. Figures 19 and 20 show extrusion cracking in 21-6-9 material. Not visible in the photographs are copper nuggets that were extruded at the end of the welds. The large amount of metal movement during confined pinch welds may act to wipe the surface clean and move contaminants out of the center weld area.

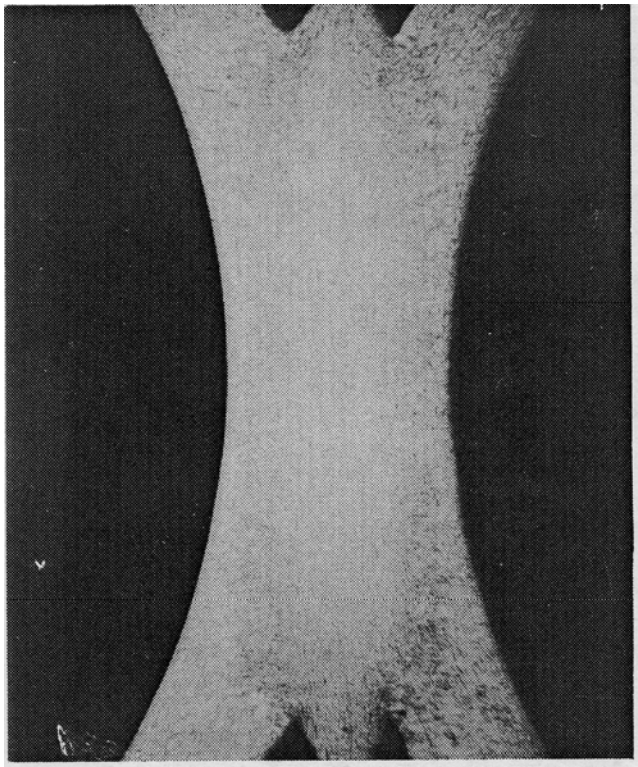

Figure 10 - SN 9148, confined pinch 304L, WD-40. (22X)

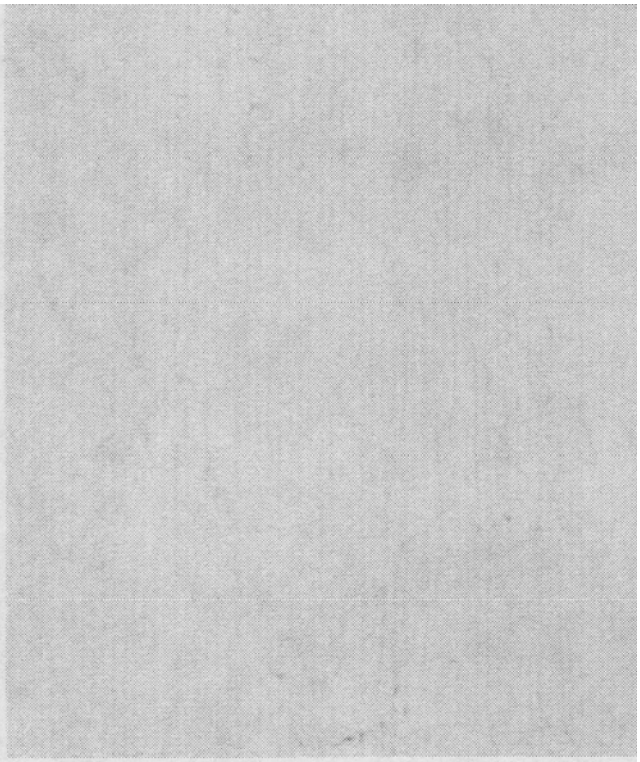

Figure 11 - SN 9148, confined pinch 304L, WD-40. (500X)

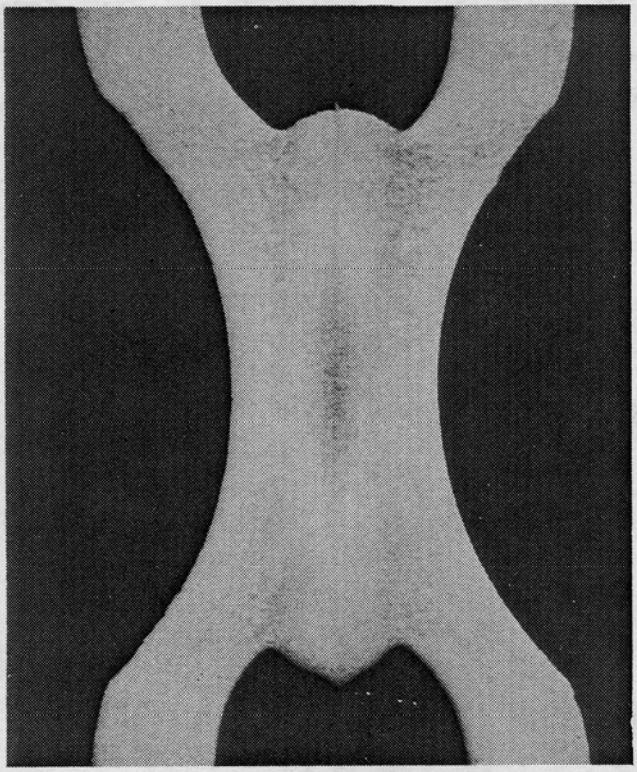

Figure 12 - SN 7582, confined pinch 21-6-9, WD-40. (22X)

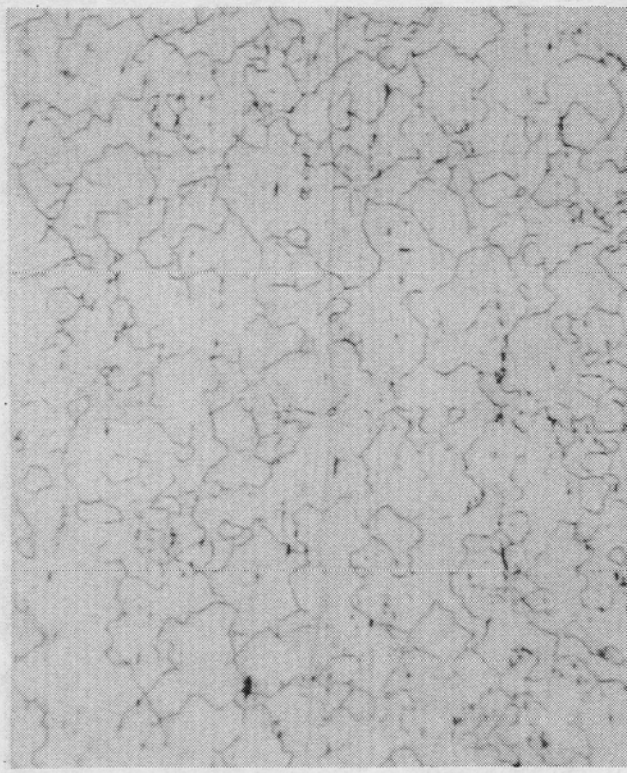

Figure 13 - SN 5782, confined pinch 21-6-9, WD-40. (500X)

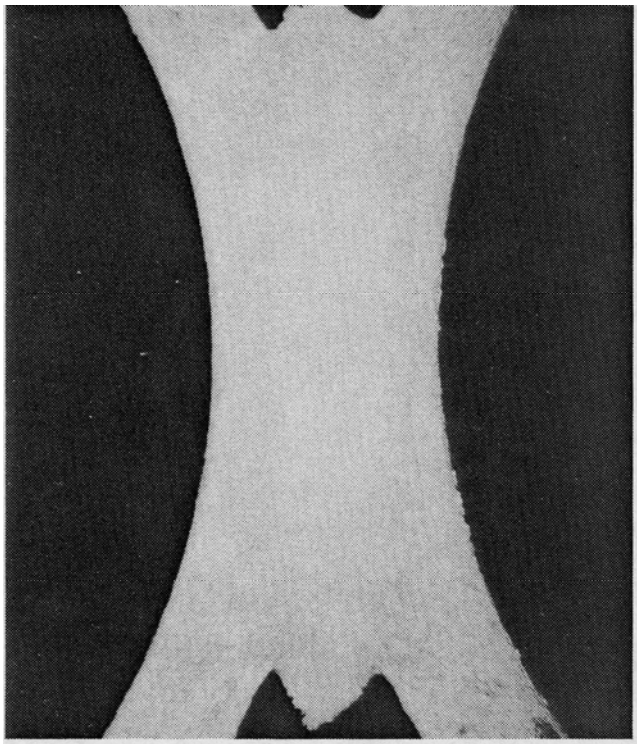

Figure 14 - SN 9135, confined pinch 304L, cotton. (22X)

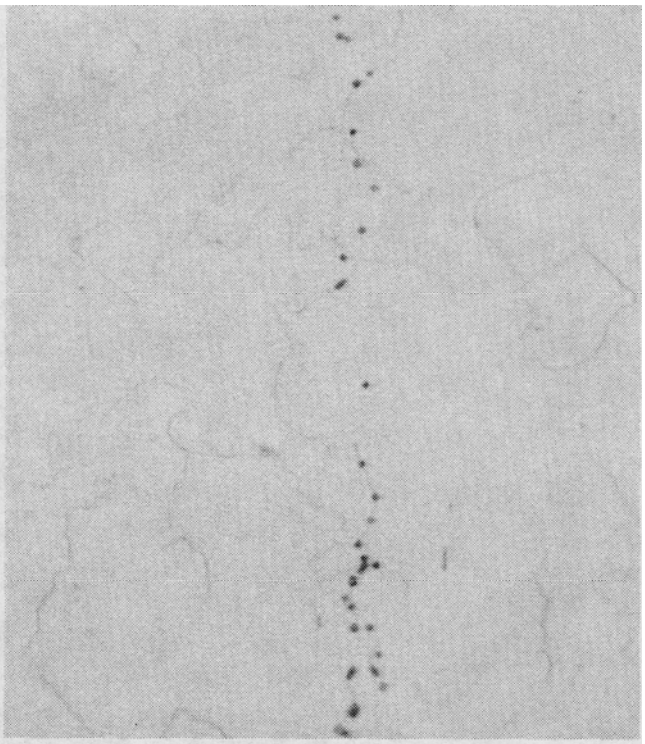

Figure 15 - SN 9135, confined pinch 304L, cotton. (500X)

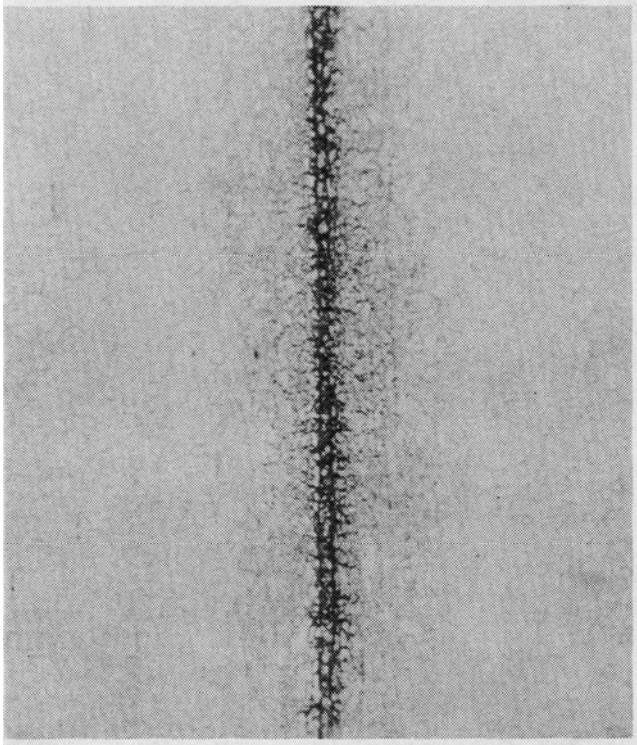

Figure 16 - SN 7579, confined pinch 21-6-9, cotton. (100X)

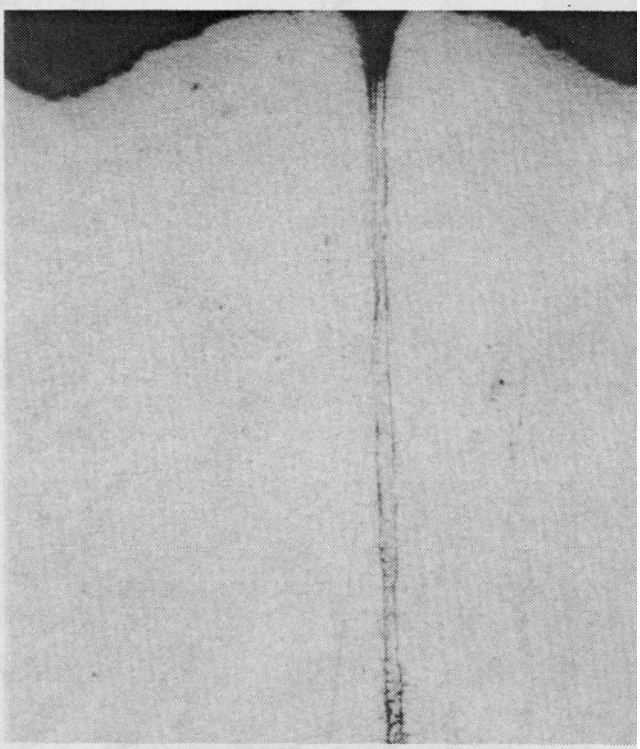

Figure 17 - SN 7579, confined pinch 21-6-9, cotton. (100X)

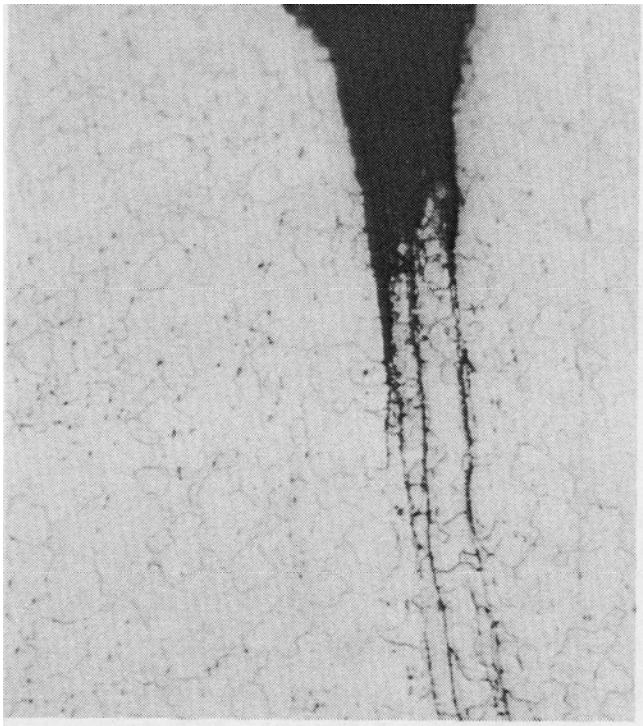

Figure 18 - SN 7579, confined pinch 21-6-9, cotton. (500X)

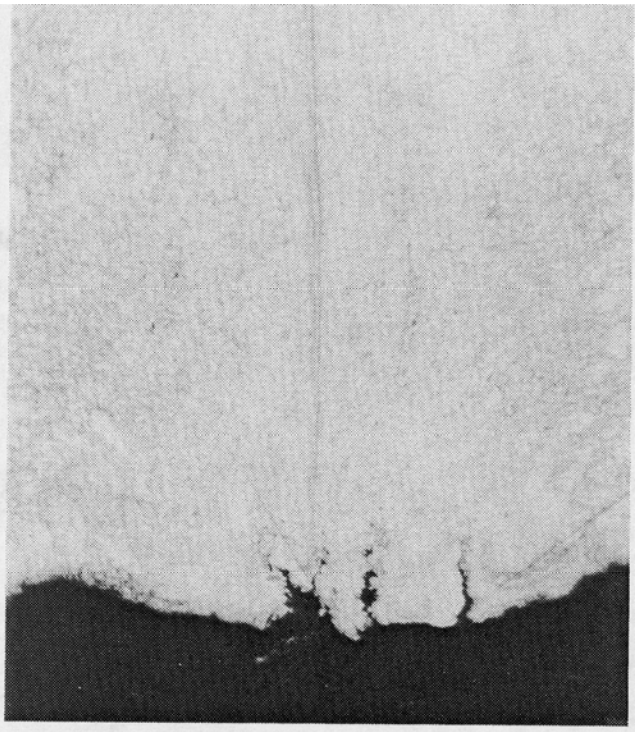

Figure 19 - SN 7578, confined pinch 21-6-9, copper. (100X)

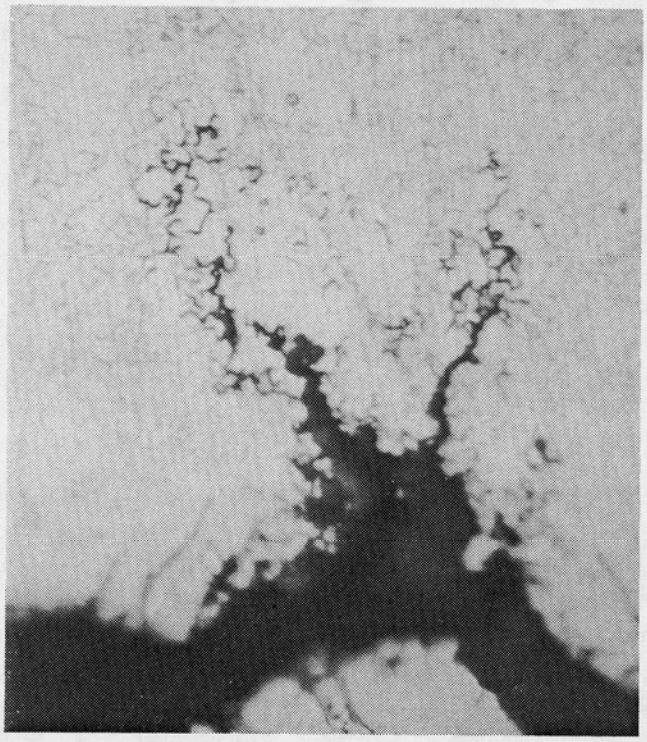

Figure 20 - SN 7578, confined pinch 21-6-9, copper. (500X)

CONTAMINANT: SILICONE VACUUM GREASE

As with the WD-40, silicone vacuum grease had little effect on bond quality. Figures 21-23 show the results on 21-6-9.

CONTAMINANT: POLYETHYLENE

The effect of polyethylene on confined pinch welds is the formation of numerous etch pits along the bond line. Figures 24-26 show results similar to those of cotton fiber. There was significant grain growth across the prior interface. Analysis of the material that is removed by etching has not yet been completed. The etch pits themselves are shaped like inverted pyramids whose "bases" appear as squares at the surface of the metal (see Figure 26).

CONTAMINANT: NYLON BRUSH BRISTLES

Nylon showed no indication of bond degradation. Figures 27-29 show the 21-6-9 weld. The only noticeable effect is the wider band of grain boundary melting. Analysis of the melted area showed only a small increase in chromium and nickel contents.

CONTAMINANT: OXIDE

The effects of oxidization varied with the material welded. Figures 30-32 show again the formation of a double bond line along the interface. Although not pictured, the oxidized tube of 304L showed the formation of a medium size weld nugget at the weld center. The increased resistance at this site was enough for localized melting to occur.

CONTAMINANT: ELECTRICAL DISCHARGE MACHINING (EDM)

Stems produced by EDM received the most extensive analysis of any contaminant. Figures 33-36 show the resulting poor bond quality. The electrode used during the EDM operation to produce the stem was copper. At first look the bond quality is a generous class 4. A deep valley is produced on etching. Evaluation prior to etching indicated a fairly good bond would exist with areas of defects as shown in Figures 35 and 36. As it turned out, the stems were coated with a copper layer from the EDM operation. Because the etchant used was electrolytic nitric acid, it is understandable that a large valley was formed. Evaluation of the contaminants in Figure 35 showed increased concentrations of chromium, oxygen, carbon, and copper.

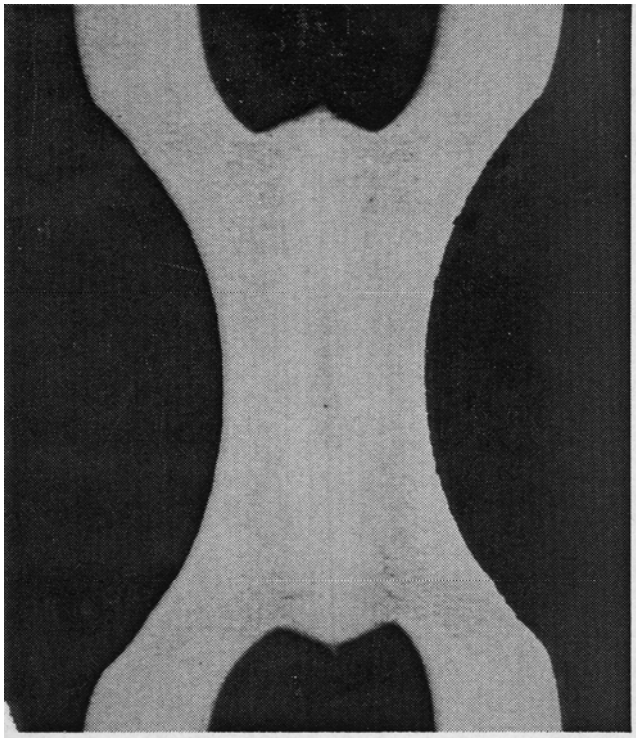

Figure 21 - SN 7583, confined pinch 21-6-9, vacuum grease. (22X)

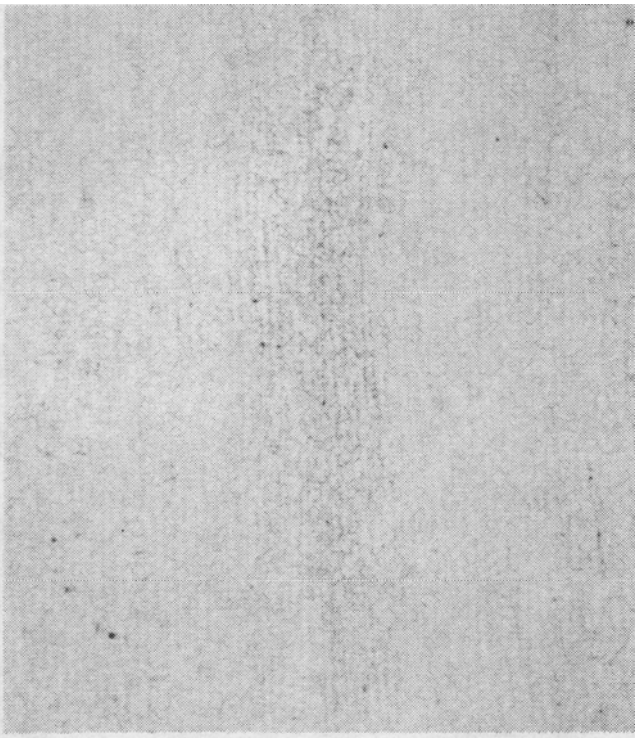

Figure 22 - SN 7583, confined pinch 21-6-9, vacuum grease. (100X)

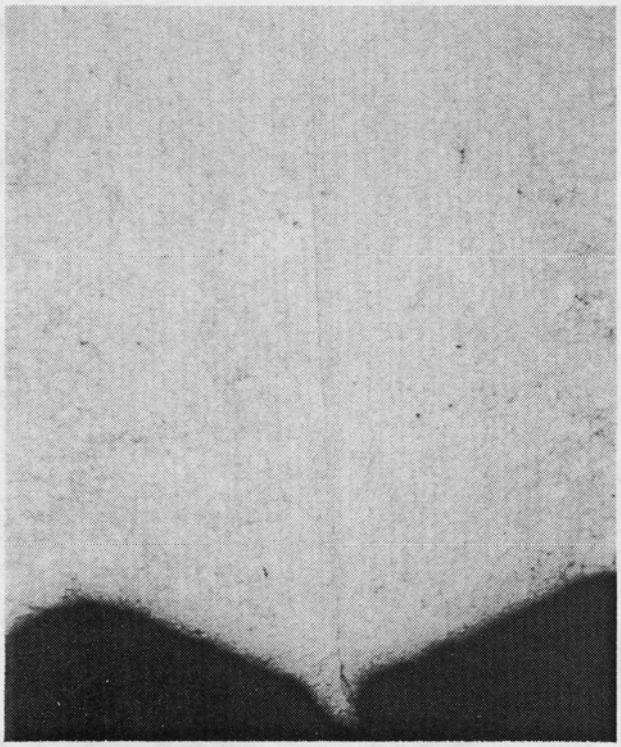

Figure 23 - SN 7583, confined pinch 21-6-9, vacuum grease. (100X)

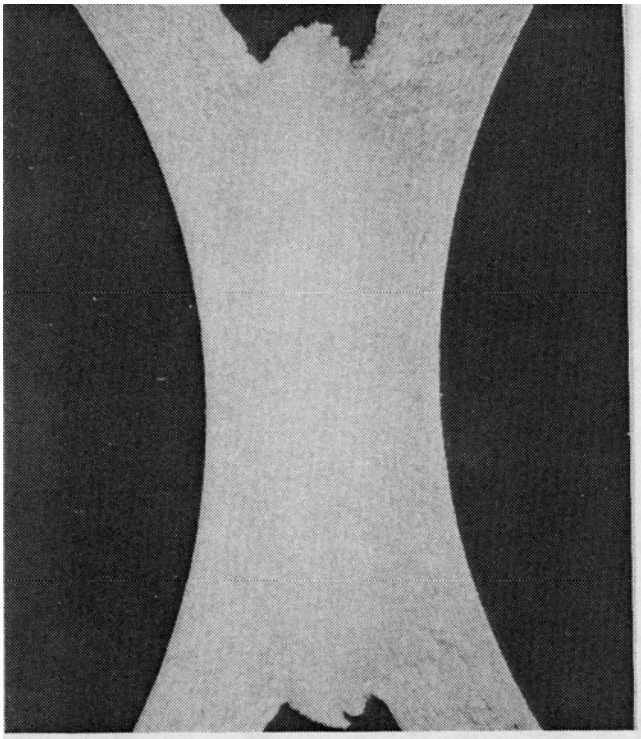

Figure 24 - SN 9138, confined pinch 304L, polyethylene. (22X)

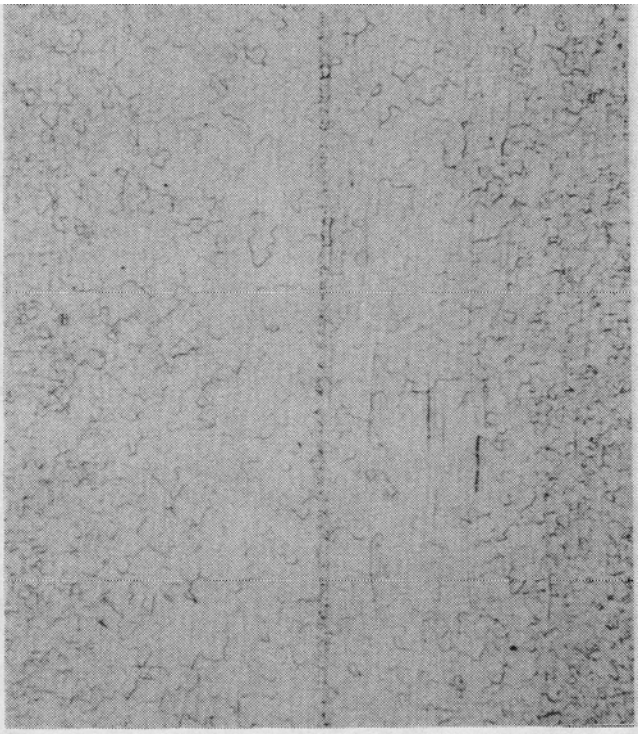

Figure 25 - SN 9138, confined pinch 304L, polyethylene. (100X)

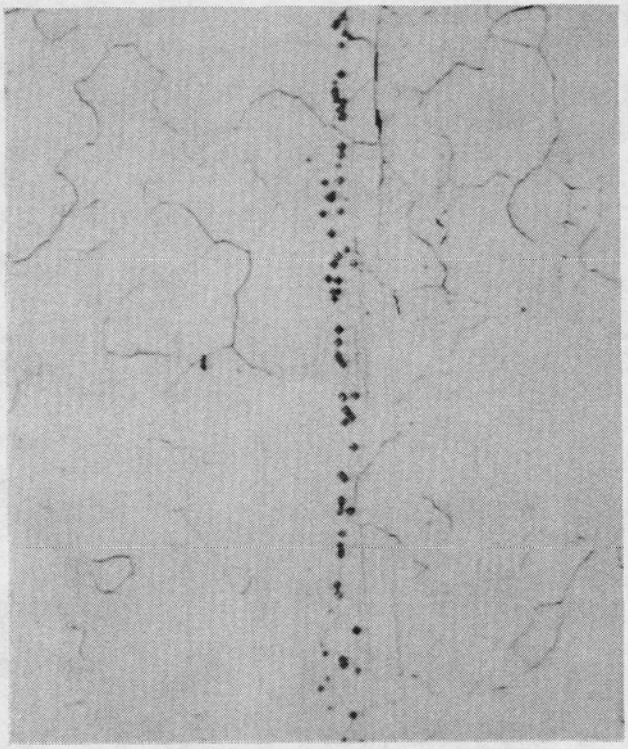

Figure 26 - SN 9138, confined pinch 304L, polyethylene. (100X)

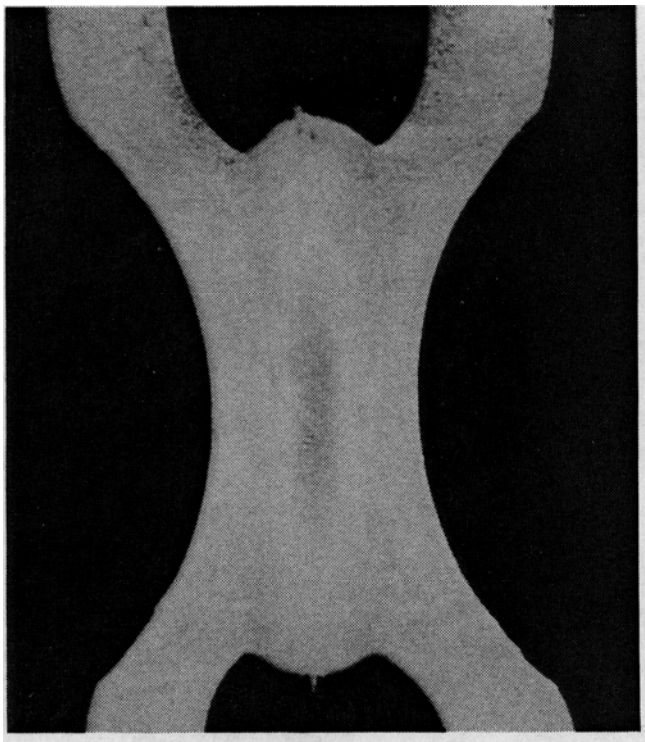

Figure 27 - SN 7581, confined pinch 21-6-9, nylon. (22X)

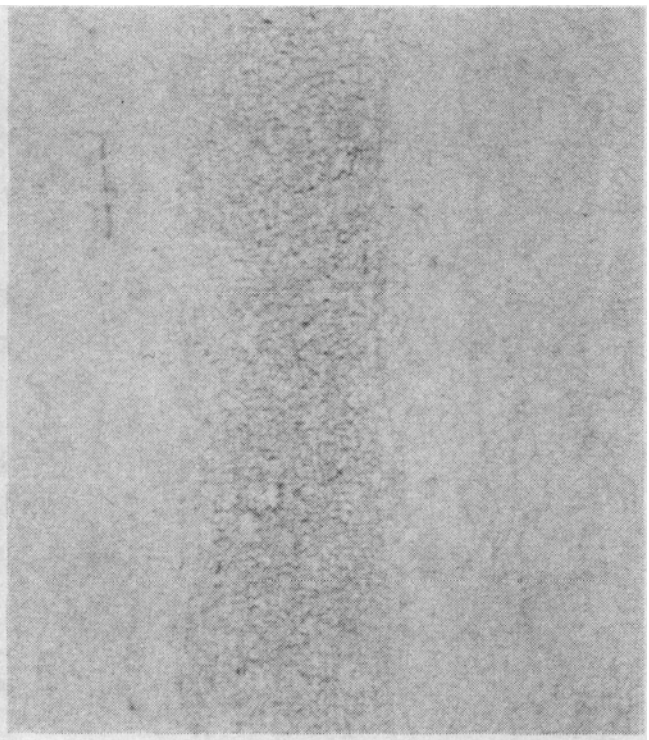

Figure 28 - SN 7581, confined pinch 21-6-9, nylon. (100X)

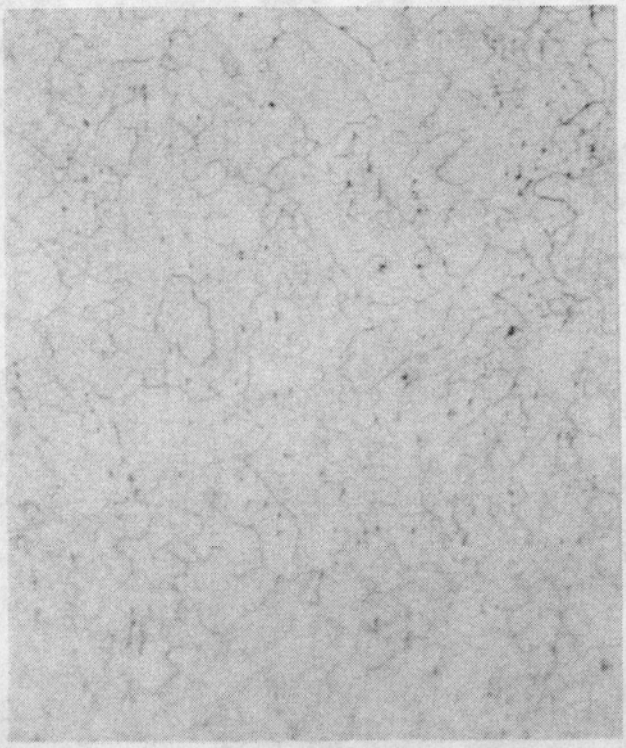

Figure 29 - SN 7581, confined pinch 21-6-9, nylon. (500X)

27a

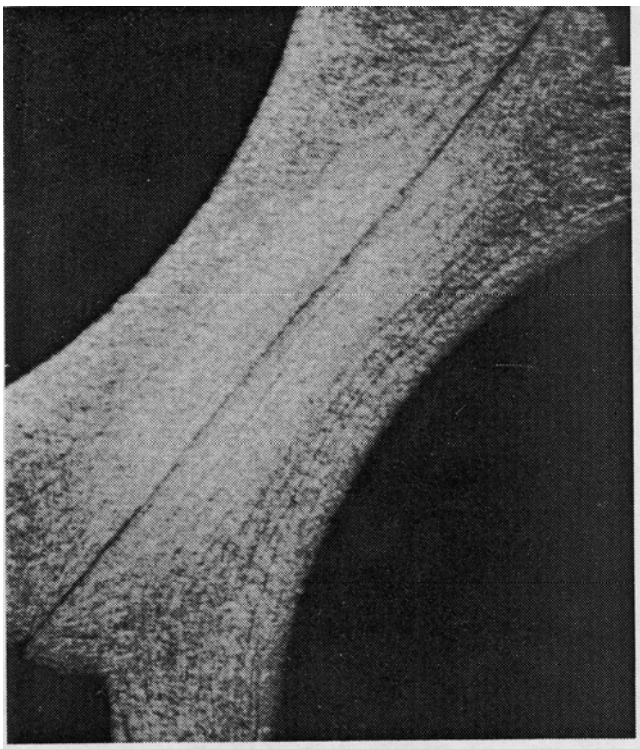

Figure 30 - SN 7584, confined pinch 21-6-9, oxide. (33X)

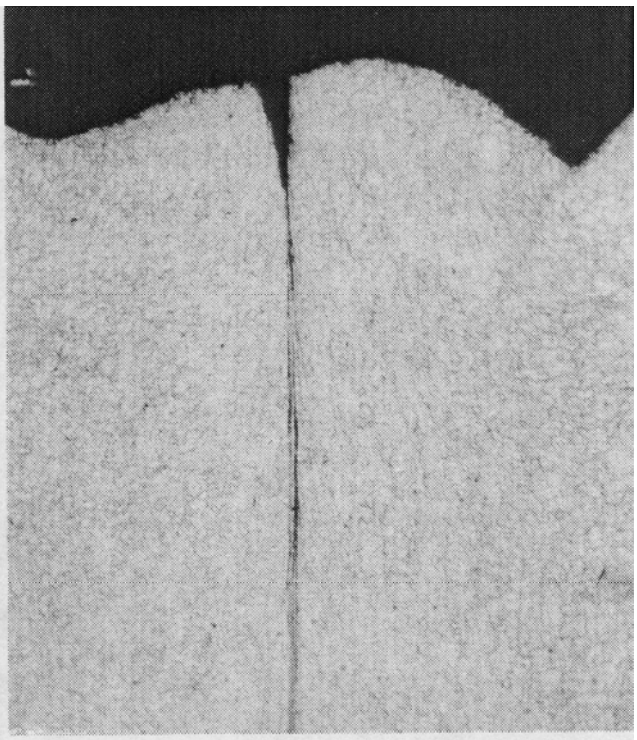

Figure 31 - SN 7584, confined pinch 21-6-9, oxide. (100X)

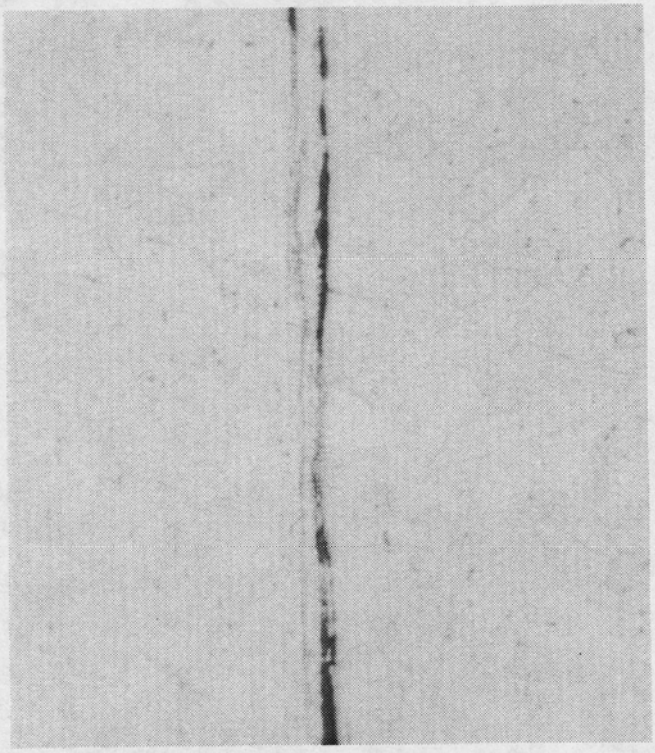

Figure 32 - SN 7584, confined pinch 21-6-9, oxide. (500X)

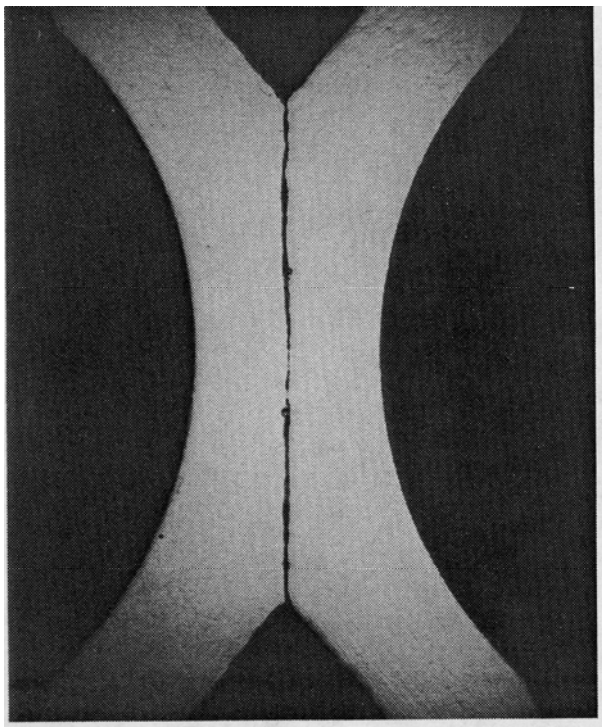

Figure 33 - SN 06001, standard pinch 304L, EDM. (22X)

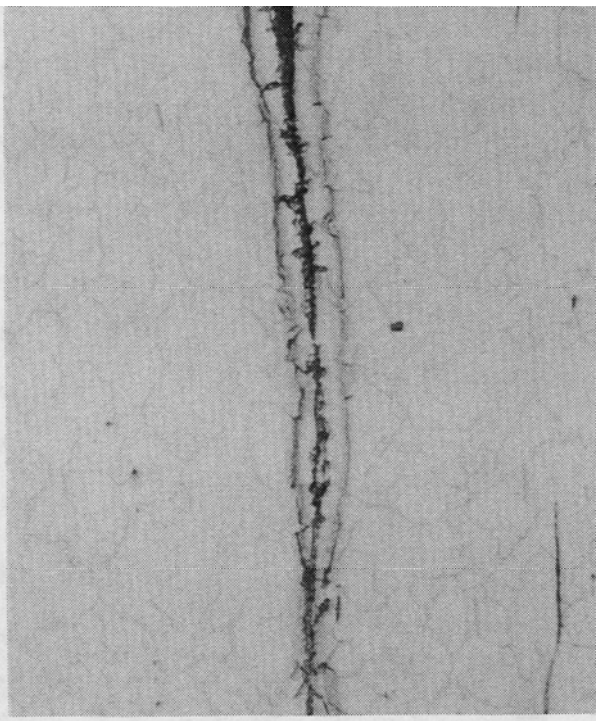

Figure 34 - SN 06001, standard pinch 304L, EDM. (500X)

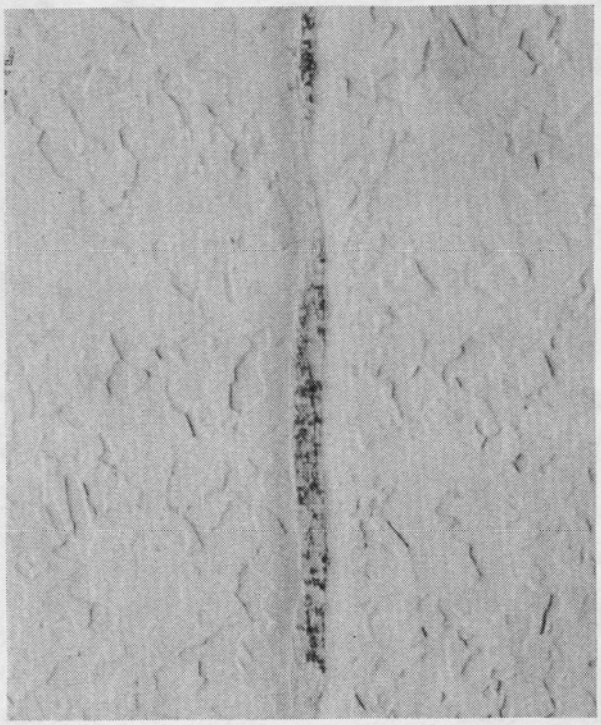

Figure 35 - SN 020002, standard pinch 304L, EDM. (460X)

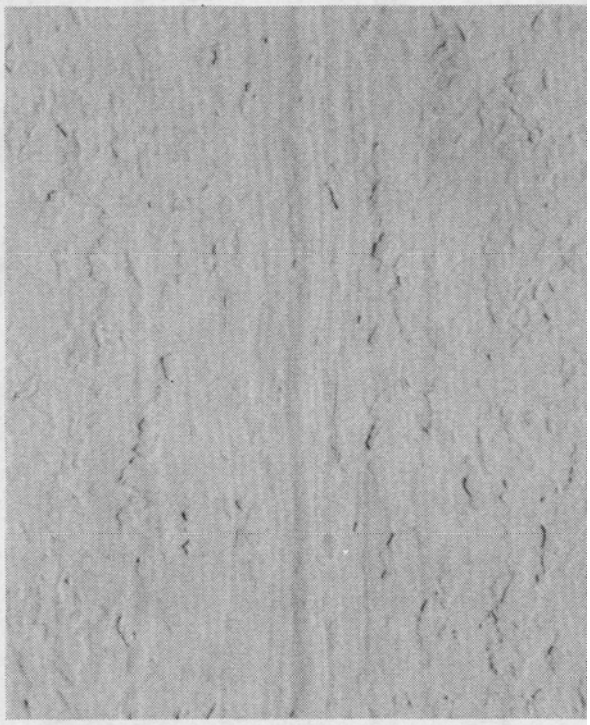

Figure 36 - SN 020002, standard pinch 304L, EDM. (460X)

Figures 37 and 38 show the inside surfaces of the stems. A very rough melted surface is evident. Figure 38 is a backscatter image with the darker areas being copper contamination.

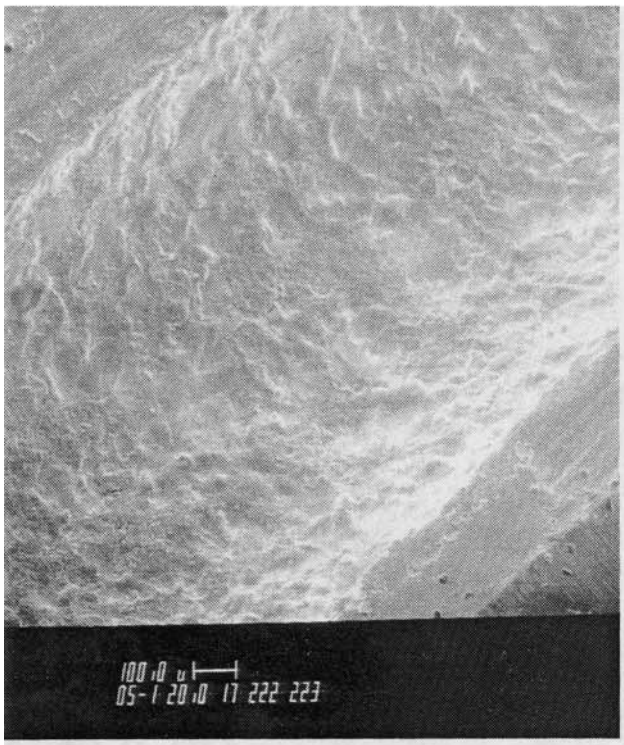

Figure 37 - SN 130001, standard pinch 304L, EDM. (50X)

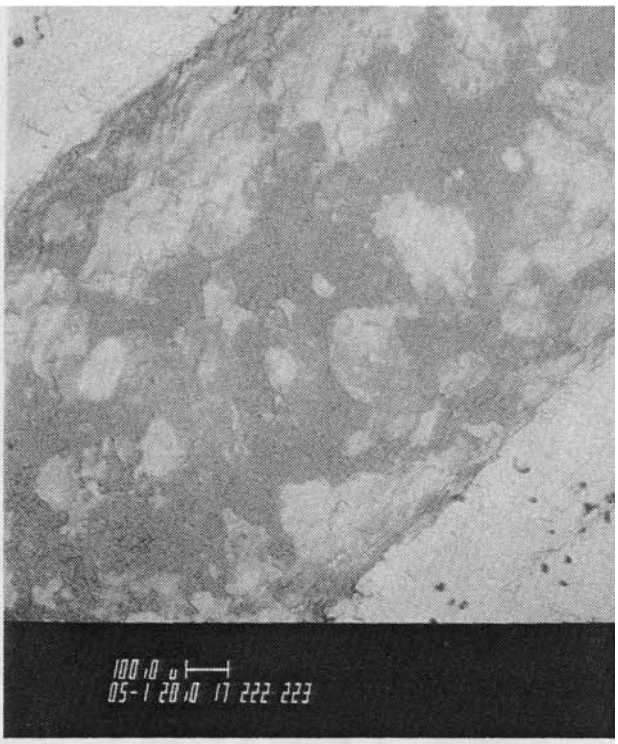

Figure 38 - SN 130001, standard pinch 304L, EDM. (50X)

An additional weld was made for peel testing after the metallurgical sectioning was completed. This weld was peel tested. Figures 45-47 show the peel surface. The weld separated cleanly at the weld interface. Evaluation showed a copper layer on both surfaces that was mostly covered with ductile dimples. Some tearing of the copper layer from the stainless steel is evident in Figure 45 and 46, indicating that a fairly good copper to copper diffusion weld had been produced.

CONCLUSIONS

The conclusions of these studies were:

- DAS could detect a larger than normal variation in secondary weld current. Oxidized stems produced much higher than normal preweld and weld resistances.

- Metallurgical evaluations of the bond qualities determined that oxide and cotton fiber contamination was the worst.

- Light materials such as silicone and WD-40 did not cause noticeable degradation.

- Polymers caused the formation of etch pits along the interface boundary.

- Copper did not cause as much cracking as expected. It also produced a higher than normal preweld resistance in 21-6-9.

- Bond quality was generally worse with 21-6-9 material than with 304L. This may be because there was less metal deformation with smaller

- EDM processing of stems was not feasible unless electrodes that did not contaminate the surface were used or the residue in the stem was removed.

This study indicated that confined pinch welds are tolerant of certain contaminants. This may be because of the higher heat content and the metal movement during welding. Unconfined welds, with lower heat input and no metal extrusion may be very susceptible to the contaminants studied. The long-term effect with respect to tritium containment is not known. It can only be surmised that it would be lower than pinch welds made on clean tubing.

REFERENCES

1. R. Harpering, "Pinch Welding Procedure Development," DuPont De Nemors Company, (December 1986). (S-RD)

2. M. A. Perkins, *Unconfined Pinch Weld Development for the W87 Vineyard*, MLM-MC-85-30-0001, Monsanto Research Corporation (October 1985), 35 pp. (C-RD)

3. "Pinch Welds, Unconfined, Microstructual Standard", SB452907, Sandia National Laboratories, Livermore, California.

4. "Pinch Welds, Unconfined, 304L Stainless Steel", SS452907, Sandia National Labortories, Livermore, California.

ACKNOWLEDGEMENTS

The authors would like to thank S. E. Moyer, W. T. Riley, W. J. Schmitz, who prepared and performed the majority of the pinch welds along with much of the physical measuring and proof testing; E. T. Kirk, manager of SROC, who supported much of the work; and M. A. Ransick, who conducted the SEM activities.

Mary J. Pacinda, Editor
Technical Publications

Distribution

Internal

1	MS9405	Bob Carling, 8700
1	MS9404	Davina Kwon, 8770
1	MS9403	Timothy Shepodd, 8778
5	MS9403	Bernice Mills, 8778
1	MS9402	Miles Clift, 08758
1	MS9221	Ed Cull, 8510
1	MS9106	Tim Gilbertson, 8226
1	MS9102	Peter Royval, 8228
1	MS9035	Charles Cadden, 8239 Dorian Balch, 8239 Nicholas Paradiso, 8239 Carl Pretzel, 8239 Steve Rice, 8239 Sean Stieper, 8239 Linh Thai, 8239 G. Ken Hicken, 8239 Peter Van Blarigan, 8239
2	MS0899	Technical Library, 4536
2	MS9018	Central Technical Files, 8944


Sandia National Laboratories